SIAM J. MATH. ANAL.
Vol. 46, No. 2, pp. 1472–1504

TRANSONIC EVAPORATION WAVES IN A SPHERICALLY SYMMETRIC NOZZLE*

XIAOBIAO LIN† AND MARTIN WECHSELBERGER‡

Abstract. This paper studies the liquid-to-vapor phase transition in a cone-shaped nozzle. Using the geometric method presented in [P. Szmolyan and M. Wechselberger, *J. Differential Equations*, 200 (2004), pp. 69–104], [M. Wechselberger and G. Pettet, *Nonlinearity*, 23 (2010), pp. 1949–1969], we further develop results on subsonic and supersonic evaporation waves in [H. Fan and X.-B. Lin, *SIAM J. Math. Anal.*, 44 (2012), pp. 405–436] to transonic waves. It is known that transonic waves do not exist if restricted solely to the slow system on the slow manifolds [H. Fan and X.-B. Lin, *SIAM J. Math. Anal.*, 44 (2012), pp. 405–436]. Thus we consider the existence of transonic waves that include layer solutions of the fast system that cross or connect to the sonic surface. In particular, we are able to show the existence and uniqueness of evaporation waves that cross from supersonic to subsonic regions and evaporation waves that connect from the subsonic region to the sonic surface and then continue onto the supersonic branch via the slow flow.

Key words. evaporation waves, blow-up technique, geometric singular perturbation theory

AMS subject classifications. 35B25, 35Q35, 34E15, 34D35, 37C50

DOI. 10.1137/120875363

1. Introduction.

In this paper, we investigate the liquid-to-vapor phase transition in a spherically symmetric cone-shaped nozzle. Subsonic evaporation processes, such as fuel injection into a combustion engine, show up in many important engineering problems and are studied in many research laboratories around the world. The ring formation observed in a shock tube experiment [33] is an example of a supersonic process, as argued by Fan in [11]. Our focus is on transonic evaporation waves. While we are not aware of any experiments where transonic evaporation waves have been observed, we expect that our theoretical results might be useful in some physical and engineering process when the speed of the fluid in a nozzle approaches sonic speed.

The study of nozzle flows was pioneered by Courant and Friedrichs [6] and Liu [26]. Transonic flow without liquid-gas phase transition has been studied by many authors; see the recent articles [3, 5, 4, 23, 35, 36]. Among them [35] dealt with subsonic and subsonic-to-sonic flows through infinitely long nozzles. For transonic flows modeled by reaction-diffusion equations, Liu and coworkers [17, 18, 27] considered one-dimensional standing waves for a simplified model of gas flows in a nozzle with general variable cross-sectional area $a(x)$. To the best of our knowledge, transonic flows that include a reaction-diffusion equation describing evaporation or condensation have not been rigorously analyzed mathematically.

Liquid-vapor phase transitions have been much studied using a van der Waals pressure function [15]. The van der Waals model requires detailed modeling of the evaporation of individual droplets [8, 30] or of the nucleation process by which vapor condenses. Figure 1(a) shows the graph of pressure p as a function of specific volume v

*Received by the editors April 30, 2012; accepted for publication (in revised form) December 26, 2013; published electronically March 25, 2014.
http://www.siam.org/journals/sima/46-2/87536.html
†Department of Mathematics, North Carolina State University, Raleigh, NC 27695-8205 (xblin@ncsu.edu). This author was partially supported by NSF grant DMS-1211070.
‡School of Mathematics and Statistics, University of Sydney, Sydney, NSW 2006, Australia (wm@maths.usyd.edu.au). This author was partially supported by ARC grants DP110102775 and FT120100309.

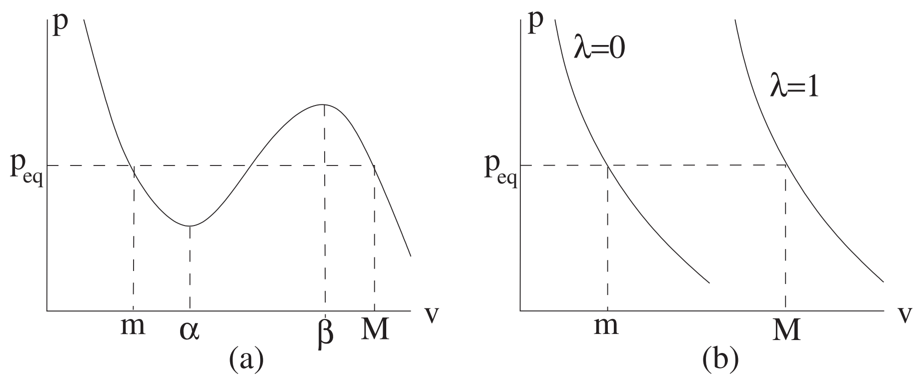

FIG. 1. (a) *shows the van der Waals pressure function* $p(v)$ *where the Maxwell line* $p = p_{eq}$ *connects* $v = m$ *to* $v = M$ *on* $p = p(v)$. (b) *shows the functions* $p(\lambda, v), \lambda = 0, 1$, *where the Maxwell line* $p = p_{eq}$ *connects* $v = m$ *on* $\lambda = 0$ *to* $v = M$ *on* $\lambda = 1$.

(the inverse of density ρ) with the temperature held constant. The decreasing branch of the pressure function p for $v < \alpha$ corresponds to the liquid state, while the other decreasing branch for $v > \beta$ corresponds to the vapor state of the fluid. There is a *spinodal region*, $\alpha < v < \beta$, in which pressure is, anomalously, an increasing function of v, i.e., a decreasing function of density ρ. This region is considered to be highly unstable and cannot be observed in experiments. In reality, this part of the pressure function p is replaced by the *Maxwell line* $p = p_{eq}$ which is defined by the "equal area rule"; see Figure 1(a). The fluid can be in any liquid/vapor state for the equilibrium pressure p_{eq}; see [9].

An alternative model proposed by Fan [9] introduces a variable $0 \le \lambda \le 1$ to represent the mass fraction of vapor, where $\lambda = 0$ represents the pure liquid state, and $\lambda = 1$ represents the pure vapor state. Since Fan's model allows intermediate values of λ, it can be used to study experiments in which mixtures of the liquid and vapor states occur [11]. In Fan's model, pressure p is a function of (λ, v). The graphs of $p(0, v)$ and $p(1, v)$ are shown in Figure 1(b). This model was motivated by, among other works, [33, 20, 31].

An important feature of Fan's model [9, 10, 11] is a reaction-diffusion equation that describes the phase transition between liquid and vapor. This model was proposed under the assumption that the heat capacity of the fluid under consideration is high (called a *retrograde fluid*), resulting in evaporation that is mainly caused by the pressure change, not the temperature change. Fan's model consists of a viscose p-system that describes the motion of compressible liquid-vapor mixture (see [22, 28]) and a reaction-diffusion equation that describes the liquid-to-vapor phase transition:

$$
\begin{aligned}
&\rho_t + \nabla \cdot (\rho u) = 0, \\
&(\rho u)_t + \nabla \cdot (\rho(uu) + p(\lambda, \rho)I) = \eta_1 \nabla \cdot (\nabla u + \nabla u^T) + \eta_2 \nabla \cdot ((\nabla \cdot u)I), \\
&(\lambda\rho)_t + \nabla \cdot (\lambda\rho u) = \frac{w(\lambda, \rho)}{\gamma} + \mu \nabla \cdot (\rho \nabla \lambda),
\end{aligned}
\tag{1.1}
$$

where $\rho > 0$ is the density of the fluid, $u \in \mathbb{R}^3$ is the velocity vector of the fluid, and $\lambda \in [0, 1]$ is the mass fraction of vapor. All the constants in (1.1) are small parameters. Among them η_1 is the shear viscosity of the fluid, η_2 is a linear combination of the

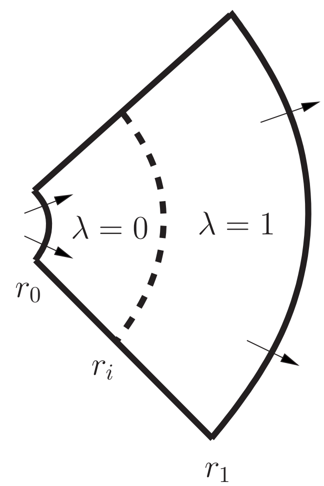

Fig. 2. *Spherically symmetric nozzle geometry: the cone's boundary is shown in solid bold. Fluid is injected at $r = r_0$ and discharged at $r = r_1$. The dashed curve at $r = r_i$ indicates an internal boundary layer of a standing evaporation wave where a transition from a liquid state ($\lambda = 0$) to a vapor state ($\lambda = 1$) happens.*

shear and the volume viscosity coefficients that is related to dilation of the fluid, and μ is the diffusion coefficient.

Assumption 1. The pressure $p(\lambda, \rho)$ is a function of the density ρ and the mass fraction of vapor λ, which satisfies

$$p_\rho > 0\,, \quad p_{\rho\rho} > 0\,, \quad p_\lambda > 0\,, \quad p(\lambda, 0) = 0\,, \quad p(\lambda, \infty) = \infty. \tag{1.2}$$

A typical pressure function which satisfies all the conditions in (1.2) is given by

$$p(\lambda, \rho) = C(1 + \lambda)\rho^k, \quad C > 0,\ k > 1\,. \tag{1.3}$$

The last equation of system (1.1) comes from a simplified model proposed by Fan [9], where the vapor initiation term has been omitted and only the vapor growth term $w(\lambda, \rho)$ is included. The function w is defined as

$$w(\lambda, \rho) := (p(\lambda, \rho) - p_{eq})\lambda(\lambda - 1)\rho, \tag{1.4}$$

and w/γ represents the vapor production rate, where γ is the typical reaction time. If $p = p_{eq}$, then $w = 0$ and the mixture could be in any liquid/vapor configuration state $0 \le \lambda \le 1$. Necessary and sufficient conditions for the existence of phase-changing traveling waves (liquid to vapor or vapor to liquid) in one-dimensional space were proved in [9, 10, 12]. Using dynamical systems methods, the proof of the existence of those one-dimensional waves was simplified in [13].

Let r be the radial coordinate of the nozzle. We assume that the fluid is injected at the smaller end $r = r_0$ and discharged at the larger end $r = r_1$ (see Figure 2). Assuming that the cone's boundary is slippery and offering no resistance to tangential flows at the boundary, the boundary effect is therefore negligible. We consider the spherically symmetric solutions which are functions of (r, t) only and satisfy the following system:

$$
(1.5)\qquad
\begin{aligned}
&\rho_t + (\rho u)_r + \frac{2\rho u}{r} = 0,\\
&(\rho u)_t + (\rho u^2 + p)_r + \frac{2\rho u^2}{r} = \epsilon \left(u_r + \frac{2u}{r} \right)_r,\\
&(\lambda\rho)_t + (\lambda\rho u)_r + \frac{2\lambda\rho u}{r} = \frac{1}{\gamma}(p - p_{eq})\lambda(\lambda - 1)\rho + \mu \left((\rho\lambda_r)_r + \frac{2\rho\lambda_r}{r} \right),
\end{aligned}
$$

where ϵ is the combined viscosity. A straightforward but rather lengthy calculation shows that $\epsilon = \eta_1 + \eta_2$.

Fan and Lin in [14] studied the existence of nontransonic evaporation waves that are in either the subsonic or supersonic region for the entire evaporation process. In this paper we shall extend their results to evaporation waves that cross the sonic surface. That is, at $r = r_0$ the liquid state fluid is subsonic (or supersonic), while at $r = r_1$ the vapor state fluid becomes supersonic (or subsonic). In what follows, we call such waves transonic evaporation waves. We look for standing waves that are stationary solutions of (1.5). The evaporation front of a stationary wave remains in the finite nozzle, making the process more useful. Assume that the fluid particles move from the smaller end to the larger end of the nozzle with the speed $u > 0$. If, in the Eulerian coordinates, the speed of the wave is zero, then in the Lagrangian coordinates the wave travels with speed $-u$, i.e., pointing towards the smaller end of the nozzle. Since the speed of sound is $\sqrt{p_\rho}$ (see, e.g., [1]), we call the standing wave with $u^2 < p_\rho$ (or $u^2 = p_\rho$ or $u^2 > p_\rho$) the subsonic (or sonic or supersonic) wave, which really means that the wave speed in the Lagrangian coordinates is subsonic (or sonic or supersonic). The region of the phase space where $u^2 < p_\rho$ (or $u^2 = p_\rho$ or $u^2 > p_\rho$) will be called the subsonic (or sonic or supersonic) region. The sonic region is a codimension one surface in the phase space.

The spherically symmetric standing waves are stationary solutions of (1.5). Based on the laws of fluid dynamics, the typical reaction time γ, the diffusion coefficient of vapor μ, and the viscosity ϵ are small parameters and are proportional to the mean free path. Using this physical fact, and to simplify the matter mathematically, we shall assume that

$$\gamma = \epsilon/a, \quad \mu = \epsilon b, \quad \text{where } a, b = O(1).$$

Then the stationary solution in spherical coordinates satisfies

$$
(1.6)\qquad
\begin{aligned}
&(\rho u)_r + \frac{2\rho u}{r} = 0,\\
&(\rho u^2 + p)_r + \frac{2\rho u^2}{r} = \epsilon \left(u_r + \frac{2u}{r} \right)_r,\\
&(\lambda\rho u)_r + \frac{2\lambda\rho u}{r} = \frac{a}{\epsilon}(p - p_{eq})\lambda(\lambda - 1)\rho + \epsilon b \left((\rho\lambda_r)_r + \frac{2\rho\lambda_r}{r} \right).
\end{aligned}
$$

In this paper we only consider an evaporation process where $p < p_{eq}$ is a necessary condition for the vapor growth function w to be positive. We state this as an assumption for future reference.

Assumption 2. The fluid described by system (1.6) satisfies the condition $p < p_{eq}$.

In the rest of the paper, we analyze this system with the emphasis on transonic evaporation waves. In particular, we look for standing waves with an internal layer

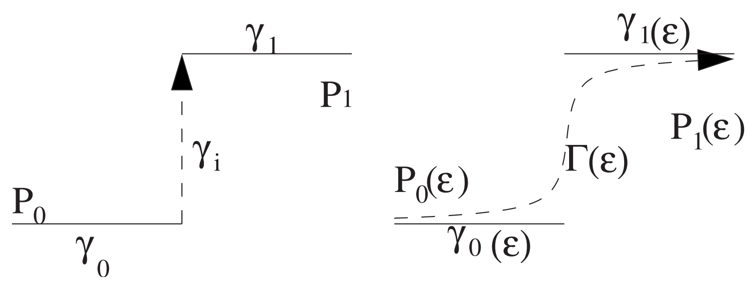

FIG. 3. *Sketch of a singular concatenated orbit* $\Gamma = \gamma_0 \cup \gamma_i \cup \gamma_1$ *and its corresponding solution* $\Gamma(\varepsilon)$.

at $r = r_i$, $r_0 < r_i < r_1$, where the transition from the liquid state to the vapor state of the fluid happens (see Figure 2). By formulating appropriate boundary conditions at the injection and discharge sites of the nozzle at $r = r_0$ and $r = r_1$, we prove the existence of unique supersonic-to-subsonic as well as subsonic-to-supersonic evaporation waves. The precise statements are given in Theorems 5.1 and 5.2 for the supersonic-to-subsonic case and in Theorem 5.3 for the subsonic-to-supersonic case.

In the following, we outline the structure of the paper that leads to the precise formulations and the proofs of these theorems. A key in our analysis is to identify system (1.6) as a singularly perturbed system. In section 2, we introduce appropriate slow and fast variables so that system (1.6) can be converted into a slow-fast dynamical system and studied by means of geometric singular perturbation theory [14, 16, 19, 34].

In section 3, we focus on the (internal) layer problem for the existence of evaporation layer solutions. In general, there may exist two kinds of evaporation transonic layer solutions connecting the pure liquid state $\lambda = 0$ to the pure vaporized state $\lambda = 1$: a supersonic-to-subsonic layer or a subsonic-to-supersonic layer. Each of these internal layers is a heteroclinic solution that crosses the sonic surface in fast radial "time." We prove that supersonic-to-subsonic internal layer solutions at $r = r_i$, $r_0 < r_i < r_1$ do exist, but subsonic-to-supersonic layer solutions do not. However, we are still able to show the existence of internal sub/supersonic-to-sonic layer solutions.

In section 4, we study the reduced outer problem on the critical manifold. We show that the flow on the critical manifold points away from the sonic surface. Thus transonic evaporation waves cannot be constructed solely by solutions on the slow manifold but must consist of internal layers.

As a common practice in singular perturbation problems, we define in section 5 singular evaporation waves $\Gamma = \gamma_0 \cup \gamma_i \cup \gamma_1$ which are concatenations of slow (outer) solutions γ_0, γ_1 and an internal layer solution γ_i (see Figure 3). As highlighted above, we are able to prove the existence and uniqueness of transonic evaporation waves $\Gamma(\varepsilon)$. In the supersonic-to-subsonic case, $\Gamma(\varepsilon)$ is $O(\varepsilon)$ close to Γ, while in the supersonic-to-subsonic case, $\Gamma(\varepsilon)$ is $O(\varepsilon^{2/3})$ close to Γ. The proof of the supersonic-to-subsonic case relies on a generalization of the exchange lemma that has been recently proven in [25]. The fractional power of the order of ε in the subsonic-to-supersonic case points to a turning point problem that stems from the sonic connection of the internal layer γ_i. To prove this result we use a geometric desingularization known as the *blow-up technique* (see [7, 21, 32]). This technique reveals an intermediate region near the sonic surface which serves as the link between the fast layer solution to the reduced flow on the slow manifold for $\varepsilon \neq 0$ (see also [2, 34]). In section 6, we outline the proof that is based on the blow-up technique (see [32] for details) and describe the flow near the sonic surface. We provide some final remarks in section 7.

2. A geometric singular perturbation approach. Since ε is a small parameter, we will use singular perturbation techniques [14, 16, 19, 34] to find standing waves for system (1.6). To convert the system into a fast-slow form, we introduce the new variables

$$m := \rho u, \quad \theta := \epsilon b \rho \lambda_y, \quad n := -mu - p + \epsilon(u_y + 2u/r), \quad r = y. \tag{2.1}$$

The dummy independent variable $y \geq 0$ allows us to rewrite (1.6) as an autonomous system. The change of variables $(\rho, u, \dot{u}, \lambda, \dot{\lambda}) \to (m, n, u, \lambda, \theta)$ is nonsingular when $u > 0$, which is the case considered in this paper. This leads to the following *slow system* on the slow scale y:

$$\begin{aligned} r_y &= 1, \\ m_y &= -\frac{2m}{r}, \\ n_y &= \frac{2mu}{r}, \\ \epsilon u_y &= n + mu + p\left(\lambda, \frac{m}{u}\right) - \epsilon\frac{2u}{r}, \\ \epsilon \lambda_y &= \frac{\theta u}{bm}, \\ \epsilon \theta_y &= \frac{\theta u}{b} - aw\left(\lambda, \frac{m}{u}\right) - \epsilon\frac{2\theta}{r}. \end{aligned} \tag{2.2}$$

An equivalent system on the fast scale $z = y/\epsilon$ is given by the *fast system*

$$\begin{aligned} r_z &= \epsilon, \\ m_z &= -\epsilon\frac{2m}{r}, \\ n_z &= \epsilon\frac{2mu}{r}, \\ u_z &= n + mu + p\left(\lambda, \frac{m}{u}\right) - \epsilon\frac{2u}{r}, \\ \lambda_z &= \frac{\theta u}{bm}, \\ \theta_z &= \frac{\theta u}{b} - aw\left(\lambda, \frac{m}{u}\right) - \epsilon\frac{2\theta}{r}. \end{aligned} \tag{2.3}$$

The singular nature of these systems is revealed by taking the limit $\epsilon \to 0$. For the fast system (2.3) this yields the *layer problem*

$$\begin{aligned} r_z = m_z = n_z = 0&, \\ u_z &= n + mu + p\left(\lambda, \frac{m}{u}\right), \\ \lambda_z &= \frac{\theta u}{bm}, \\ \theta_z &= \frac{\theta u}{b} - aw\left(\lambda, \frac{m}{u}\right) \end{aligned} \tag{2.4}$$

for the evolution of the fast variables (u, λ, θ). Note that the slow variables (r, m, n) are parameters in the layer problem. On the other hand, for the slow system (2.2) the result of taking the limit $\epsilon \to 0$ is the *reduced problem*

$$
\begin{aligned}
r_y &= 1, \\
m_y &= -\frac{2m}{r}, \\
n_y &= \frac{2mu}{r}, \\
0 &= n + mu + p\left(\lambda, \frac{m}{u}\right), \\
0 &= \frac{\theta u}{bm}, \\
0 &= \frac{\theta u}{b} - aw\left(\lambda, \frac{m}{u}\right),
\end{aligned} \tag{2.5}
$$

which is a differential-algebraic system for the evolution of the slow variables (r, m, n). The phase space of the reduced problem is defined by the algebraic constraints

$$
\begin{aligned}
0 &= n + mu + p\left(\lambda, \frac{m}{u}\right), \\
0 &= \frac{\theta u}{bm}, \\
0 &= \frac{\theta u}{b} - aw\left(\lambda, \frac{m}{u}\right),
\end{aligned} \tag{2.6}
$$

or equivalently

$$
\begin{aligned}
n &= -mu - p\left(\lambda, \frac{m}{u}\right), \\
\theta &= 0, \\
w\left(\lambda, \frac{m}{u}\right) &= 0\,.
\end{aligned} \tag{2.7}
$$

Assuming $\rho > 0$, it follows that $w = 0$ has three possible solutions, $\lambda = 0$, $\lambda = 1$, and $p = p_{eq}$, which correspond to the three branches of the three-dimensional *critical manifold* (or slow manifold in some of the literature) $S = S_0 \cup S_1 \cup S_e$. These branches can be expressed as functions of the (r, m, u) variables:

$$
S_{0,1,e} := \{(r, m, n, u, \lambda, \theta) \in \mathbb{R}^6 \,:\, \lambda = \Lambda(m, u),\, \theta = 0,\, n = N(m, u)\}\,. \tag{2.8}
$$

Under Assumption 2, the surface S_e will not be of interest to us. The functions $\Lambda(m, u)$ and $N(m, u)$ for S_0 and S_1 are given in the following table:

	$\Lambda(m, u)$	$N(m, u)$
S_0	0	$-mu - p(0, m/u)$
S_1	1	$-mu - p(1, m/u)$

An example of the graphs of S_0 and S_1 is shown in Figure 4, where we chose $p = (1 + \lambda)\rho^2$ as a representative pressure function in (1.3). For fixed (λ, m), since the function $p(\lambda, m/u)$ is concave upward with $p(\lambda, 0) = 0, p(\lambda, \infty) = \infty$, the graph of $N(m, u)$ is concave downward, has a vertical asymptote as $u \to 0$, and approaches $n = -mu$ as $u \to \infty$. The maximum value of $N(m, u)$ is reached on the codimension one sonic surface where $u^2 = p_\rho$.

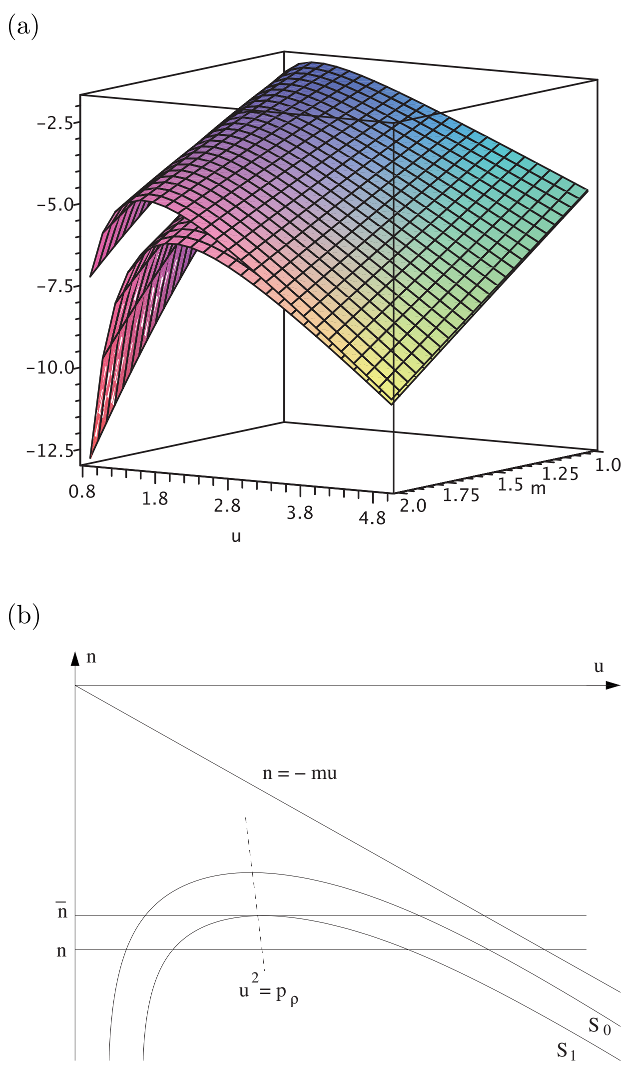

Fig. 4. (a) *Shown are functions* $n = N(m, u)$ *for the branches* S_0, S_1 (2.8) *of the three-dimensional critical manifold* S. *Here we use* $p(\lambda, \rho) = (1 + \lambda)\rho^2$ *for numerical computations. Note that* S_0 *lies above* S_1. (b) *Cross section for a fixed* m*: If* $n < \bar{n}$*, there are four equilibrium points: two on* S_0 *and two on* S_1. *If* $n = \bar{n}$*, there are three equilibrium points: two on* S_0 *and one on* S_1.

Definition 1. *For a fixed* m*, let* $\bar{n}$ *be the maximum value of* $N(m, u)$ *on* S_1.

For a given pair of m and r, the number of equilibrium points of the layer problem on S_0 or S_1 is a function of n only. Since equilibria do not depend on r, we will often not mention r in the future. There is no equilibrium point on S_1 for $n > \bar{n}$. Therefore we shall only consider $n \leq \bar{n}$. Depending on $n = \bar{n}$ or $n < \bar{n}$, the number of equilibrium points on $S_0 \cup S_1$ can be three or four as illustrated in Figure 4.

From the layer problem (2.4) we find that

$$u_z = n + mu + p\left(\lambda, \frac{m}{u}\right) = n - N(m, u). \tag{2.9}$$

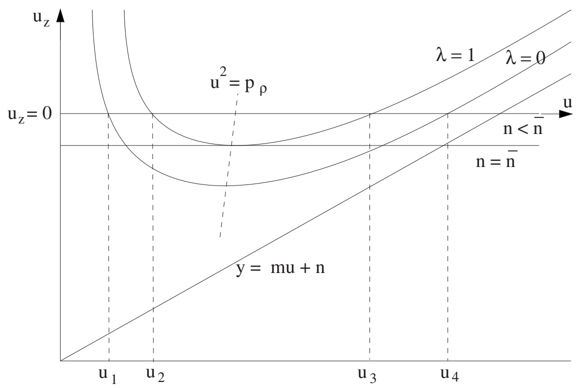

FIG. 5. *The two concave-up curves correspond to $n = -N(m, u)$ with $\lambda = 0, 1$, respectively. By choosing $\lambda \in [0, 1]$ and u, we can find u_z from the figure. For example, given $n < \bar{n}$, we have $u_z < 0$ if $u_2 < u < u_3$ and $u_z > 0$ if $u < u_1$ or $u > u_4$.*

By flipping the graph of $N(m, u)$ to $-N(m, u)$ and then shifting by the constant n, we can easily determine the sign of u_z for any (λ, u); see Figure 5. This will be very useful when constructing the layer solutions.

2.1. Stability analysis of the layer problem. We study the eigenvalues and eigenfunctions for the equilibrium points of the layer problem (2.4) on $S_0 \cup S_1$. The Jacobian of (2.4) is given by

$$J = \begin{pmatrix} m + p_u & p_\lambda & 0 \\ \frac{\theta}{bm} & 0 & \frac{u}{bm} \\ \frac{\theta}{b} - aw_u & -aw_\lambda & \frac{u}{b} \end{pmatrix} . \tag{2.10}$$

The derivatives of p and w with respect to λ and u are given in the following table:

	p_u	p_λ	w_u	w_λ
S_0	$-\frac{m}{u^2}p_\rho < 0$	> 0	0	$-\frac{m}{u}(p - p_{eq})$
S_1	$-\frac{m}{u^2}p_\rho < 0$	> 0	0	$+\frac{m}{u}(p - p_{eq})$

On the branches S_0 and S_1, the Jacobian reduces to

$$J = \begin{pmatrix} \frac{m}{u^2}(u^2 - p_\rho) & p_\lambda & 0 \\ 0 & 0 & \frac{u}{bm} \\ 0 & \pm a\frac{m}{u}(p_{eq} - p) & \frac{u}{b} \end{pmatrix} , \tag{2.11}$$

where the minus sign is associated to S_0 and the plus sign to S_1. The eigenvalues $\{l_1, l_2, l_3\}$ of the matrix J satisfy the characteristic equation

$$\left(\frac{m}{u^2}(u^2 - p_\rho) - l\right) \cdot \left(l\left(l - \frac{u}{b}\right) \pm \frac{a}{b}(p - p_{eq})\right) = 0 \, , \tag{2.12}$$

where the minus sign belongs to S_1 and the plus sign to S_0. On both branches S_0, S_1, one eigenvalue is given by $l_1 = \frac{m}{u^2}(u^2 - p_\rho)$. On the branch S_1 and under Assumption 2, $p < p_{eq}$, the other two eigenvalues are real and satisfy $l_2 < 0 < l_3$. On the other branch S_0, if $p < p_{eq}$ and $u^2 + 4ab(p - p_{eq}) > 0$, then the other two eigenvalues are real and satisfy $0 < l_2 < l_3$. On the other hand, if $p < p_{eq}$ and $u^2 + 4ab(p - p_{eq}) < 0$, the eigenvalues l_2, l_3 are complex conjugates. A direct calculation of the corresponding eigenspace of this complex conjugate pair of eigenvalues $\{l_2, l_3\}$ implies that layer solutions will enter the physically unrealistic region $\lambda < 0$ as $z \to -\infty$, due to the oscillations of these layer solutions near S_0 caused by the complex eigenvalues.

The evaporation waves discussed in this paper occur in a bounded subset Ω of the phase space, defined as

$$\Omega := \{(r, m, n, u, \lambda, \theta) : \bar{u} \leq u \leq \bar{\bar{u}},\ \bar{m} \leq m \leq \bar{\bar{m}},\ r_0 \leq r \leq r_1\}.$$

The set Ω and the positive constants $\bar{u}$, $\bar{\bar{u}}$, $\bar{m}$, and $\bar{\bar{m}}$ depend on the types of evaporation waves we try to construct and are not difficult to determine in each case. Throughout this paper we assume that the variables (u, λ, m) satisfy the following condition.

Assumption 3. $u^2 + 4ab(p(\lambda, \frac{m}{u}) - p_{eq}) > 0$ for $\bar{u} \leq u \leq \bar{\bar{u}}$, $\bar{m} \leq m \leq \bar{\bar{m}}$, and $\lambda = 0$.

Although this assumption is only given for $\lambda = 0$, it is easy to show the following result.

LEMMA 2.1. *If* $(u, \lambda = 0, m)$ *satisfy Assumption* 3, *then* $u^2 + 4ab(p(\lambda, \frac{m}{u}) - p_{eq}) > 0$ *for* $0 \leq \lambda \leq 1$.

Proof. Since $p_\lambda > 0$, then we have $p(\lambda, m/u) > p(0, m/u)$ for $\lambda > 0$. ▯

Notice that if $\bar{u} > 0$ is given, Assumption 3 holds if a and b are small enough such that $ab < \bar{u}^2/(4p_{eq})$.

Under Assumption 3, the eigenvalues of the Jacobian (2.11) are real. The corresponding eigenvectors to the eigenvalues $\{l_1, l_2, l_3\}$ are given by

$$v_1 = (1, 0, 0), \quad v_j = \left(\frac{p_\lambda}{l_j - l_1}, 1, \frac{bm}{u} l_j\right), \ j = 2, 3, \tag{2.13}$$

where we assume that $l_j \neq l_1, j = 2, 3$, for convenience. We remark that if $l_1 = l_j$ for $j = 2$ or 3, then the expression for v_j can be complicated. However, most of the results of this paper do not depend on this expression and are still valid.

An important observation is that the eigenvalue l_1 vanishes if $u^2 = p_\rho$, i.e., along the sonic surface of S_0, respectively, S_1. Geometrically, the branches S_0 and S_1 are three-dimensional folded manifolds within the six-dimensional phase space where the sonic surface corresponds to the fold where the layer flow is tangent to the branches S_0 and S_1 along the eigendirection spanned by the nullvector v_1. Consequently, the layer problem projected onto the one-dimensional nullspace undergoes a saddle-node bifurcation along the sonic surface, as can be seen in Figure 4.

Under Assumptions 2 and 3, the signs of the eigenvalues for the layer problem on S_0 and S_1 can be summarized in the following table:

	S_0	S_1
subsonic, $u^2 < p_\rho$	$-, +, +$	$-, -, +$
sonic, $u^2 = p_\rho$	$0, +, +$	$0, -, +$
supersonic, $u^2 > p_\rho$	$+, +, +$	$+, -, +$

Since the critical manifolds consist of equilibrium points of the layer problem, the fiber dimensions of the associated unstable and stable manifolds of S_0 and S_1 on the subsonic and supersonic regions, and the center(-stable) manifolds of S_0 and S_1 on the sonic surface, can be determined by the signs of eigenvalues of the layer problem and are listed in the following table:

	dim $W^u(S_0)$	dim $W^s(S_0)$	dim $W^u(S_1)$	dim $W^s(S_1)$
subsonic	2	1	1	2
supersonic	3	0	2	1
sonic		dim $W^c(S_0) = 1$		dim $W^{cs}(S_1) = 2$

3. Existence of evaporation layer solutions. Evaporation layer solutions are heteroclinic connections from S_0 to S_1. Assuming that Assumptions 2 and 3 are satisfied, then the types of connections are listed in the following table, where we refer to the fiber dimensions of S_0 and S_1:

	dim $W^u(S_0) \to$ dim $W^{(c)s}(S_1)$
subsonic	$2 \to 2$
supersonic	$3 \to 1$
transonic (sub to super)	$2 \to 1$
transonic (super to sub)	$3 \to 2$
sub (or supersonic) to sonic	$2 \to 2$ (or $3 \to 2$)

The existence of nontransonic evaporation waves, i.e., subsonic-to-subsonic and supersonic-to-supersonic waves, has been proved in [14], where the transverse intersection of $W^u(S_0)$ and $W^s(S_1)$ for subsonic waves was checked numerically. Using the method presented in the proof of Theorem 3.3, it can also be proved rigorously.

Definition 2. *For any $0 < \alpha < \beta$, a corresponding rectangle $R(\alpha, \beta)$ can be defined in the (u, λ)-plane:*

$$R(\alpha, \beta) := \{(u, \lambda) | 0 \leq \lambda \leq 1,\ \alpha \leq u \leq \beta\}.$$

A pentahedron-shaped solid W (Figure 6) in (u, λ, θ)-space is said to be based on the rectangle $R(\alpha, \beta)$ if the five surfaces of W are as follows:

$$\begin{aligned} F_b &= \{(u, \lambda, \theta) : \alpha < u < \beta\,, 0 < \lambda < 1\,, \theta = 0\}, \\ F_r &= \{(u, \lambda, \theta) : \alpha < u < \beta\,, \lambda = 1\,, 0 < \theta < m/2\}, \\ F_s &= \{(u, \lambda, \theta) : \alpha < u < \beta\,, 0 < \lambda < 1\,, \theta = m\lambda/2\}, \\ F_k &= \{(u, \lambda, \theta) : u = \beta\,, 0 < \lambda < 1\,, 0 \leq \theta \leq m\lambda/2\}, \\ F_f &= \{(u, \lambda, \theta) : u = \alpha\,, 0 < \lambda < 1\,, 0 < \theta < m\lambda/2\}. \end{aligned} \tag{3.1}$$

Lemma 3.1. *For a given m, assume that (u, λ, m) satisfy Assumption 2 for $\alpha \leq u \leq \beta$. If W is a pentahedron-shaped solid based on the rectangle $R(\alpha, \beta)$, then at points on the planes F_b, F_r, and F_s, the flow of the layer problem (2.4) leaves W.*

Moreover, if $(\alpha, 0, 0)$ and $(\beta, 0, 0)$ are two equilibrium points for the layer problem on S_0, then at points on the plane F_f, the flow of the layer problem (2.4) enters W, while at points on the plane F_k, the flow of the layer problem (2.4) leaves W.

Proof. We show that the layer flow leaves W through the interior of F_x, $x = b, r, s$, i.e., $g \cdot n_x > 0$ evaluated in the interior of F_x, where g denotes the vector field of the layer problem (2.4) and n_x denotes the corresponding outer normal vector of F_x given by

$$n_b = (0, 0, -1), \quad n_r = (0, 1, 0), \quad n_s = (0, -m/2, 1). \tag{3.2}$$

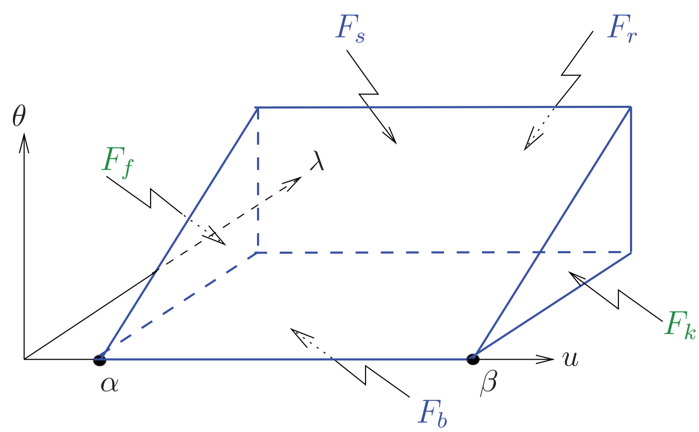

FIG. 6. *The pentahedron that is based on the rectangle* $R(\alpha, \beta)$ *and all its surfaces* F_x, $x = b, f, k, r, s$.

We have the following results for $p < p_{eq}$:

$$
\begin{aligned}
(n_b \cdot g)|_{F_b} &= aw\left(\lambda, \frac{m}{u}\right) > 0\,, \quad \alpha < u < \beta\,, 0 < \lambda < 1,\\
(n_r \cdot g)|_{F_r} &= \frac{\theta u}{bm} > 0\,, \quad \alpha < u < \beta\,, \theta > 0,\\
(n_s \cdot g)|_{F_s} &= \frac{\lambda m u}{4b} - a(p - p_{eq})\lambda(\lambda - 1)\frac{m}{u} = \frac{\lambda m}{4bu}\left(u^2 - 4ab(p - p_{eq})(\lambda - 1)\right)\\
&\geq \frac{\lambda m}{4bu}\left(u^2 + 4ab(p - p_{eq})\right) > 0\,, \quad \alpha < u < \beta\,, 0 < \lambda < 1,
\end{aligned}
$$

which follows from Assumption 3 and Lemma 2.1.

The outer normal vectors of F_k and F_f are $n_k = (1, 0, 0)$, $n_f = (-1, 0, 0)$, respectively. We have $n + mu + p = 0$ at the equilibria $(\alpha, 0, 0)$ and $(\beta, 0, 0)$. Due to the fact that $p_\lambda > 0$ and $\lambda > 0$, we have

$$
\begin{aligned}
(n_f \cdot g)|_{F_f} &= (-n - mu - p)|_{F_f} < 0, \quad \theta > 0\,, 0 < \lambda < 1,\\
(n_k \cdot g)|_{F_k} &= (n + mu + p)|_{F_k} > 0, \quad \theta > 0\,, 0 < \lambda < 1.
\end{aligned}
$$

This proves the last assertion of the lemma. ◻

We should always assume that $n \leq \bar{n}$ (otherwise, evaporation layers are not possible). If $n < \bar{n}$, then there are two equilibrium points $E_-^1, E_-^2 \in S_0$ and two equilibrium points $E_+^1, E_+^2 \in S_1$. Also E_-^1, E_+^1 are on the subsonic and E_-^2, E_+^2 are on the supersonic branches, respectively. If $n = \bar{n}$, there are two equilibrium points $E_-^1, E_-^2 \in S_0$ and a unique equilibrium point $E_+ \in S_1$. Also E_-^1, E_+, E_-^2 are on the subsonic, sonic, and supersonic branches, respectively; see Figures 7 and 8. The signs of u_z can easily be determined from these figures as well, as described in section 2. Let us define the u-nullsurface in the (u, λ, θ)-space along which $u_z = 0$ in (2.9). Since $p_\lambda > 0$ it follows that $u_z = 0$ can be solved for $\lambda = \Lambda^c(u)$. Furthermore, we know that

$$
\frac{d\Lambda^c}{du} = \frac{m}{u^2}\frac{(p_\rho - u^2)}{p_\lambda}
\begin{cases}
> 0 \text{ if } u^2 < p_\rho,\\
= 0 \text{ if } u^2 = p_\rho,\\
< 0 \text{ if } u^2 > p_\rho.
\end{cases}
$$

Note that the right-hand side of (2.9) is independent of θ. Hence, we can define the projection of a u-nullsurface along the θ-direction, onto (u, λ)-space, and call it a u-nullcline. For simplicity we sometimes call such a u-nullsurface a u-nullcline too. In Figures 7(b) and 8(b), curves in (u, λ)-space connecting equilibrium points diagonally inside the rectangle boxes are segments of the u-nullcline.

If $n < \bar{n}$, then there are two trivial transonic heteroclinic orbits from supersonic to subsonic regions: One satisfies $\lambda = 0, \theta = 0$ and connects E_-^2 to E_-^1 on S_0; the other satisfies $\lambda = 1, \theta = 0$ and connects E_+^2 to E_+^1 on S_1. Following the terminology of Fan [11], we will call them *wet shock* and *dry shock*. With (λ, θ) given, a wet or dry shock is determined by a scalar ODE for $u(z)$ and is easy to find. From Figures 7 and 8, it is clear that $u_z < 0$ for all $z \in \mathbb{R}$ for both wet shocks and dry shocks. If $n = \bar{n}$, there is only one trivial transonic heteroclinic orbit connecting E_-^2 to E_-^1 on S_0, which is a wet shock. All those trivial transonic layers are monotone decreasing in u and go from supersonic to subsonic regions.

3.1. Existence of supersonic-to-subsonic layer solutions. For $n < \bar{n}$, there are four equilibrium points $\{E_-^1, E_+^1, E_+^2, E_-^2\}$ on $S_0 \cup S_1$ marked by their u coordinates $u_-^1 < u_+^1 < u_+^2 < u_-^2$ in Figure 7.

THEOREM 3.1. *Assume $n < \bar{n}$ and that Assumptions 2 and 3 are satisfied with $\bar{u} < u_-^1 < u_-^2 < \bar{\bar{u}}$. Then there exists a one-parameter family of supersonic-to-subsonic heteroclinic solutions to the layer problem (2.4) connecting E_-^2 to E_+^1 (see Figure 7). This one-parameter family of $E_-^2 \to E_+^1$ heteroclinic solutions is bounded by two pairs of heteroclinic solutions. At one end the boundary is a pair of heteroclinic orbits connecting E_-^2 to E_-^1 along the line $\lambda = 0$ (wet shock) and then connecting E_-^1 to E_+^1 (subsonic layer). At the other end the boundary is a pair of heteroclinic orbits connecting E_-^2 to E_+^2 (supersonic layer) and then connecting E_+^2 to E_+^1 along the line $\lambda = 1$ (dry shock).*

Proof. Among the u-coordinates of the four equilibrium points, u_-^1 is the minimum and u_-^2 is the maximum. Based on the two-dimensional rectangle $R(u_-^1, u_-^2)$, one can construct a pentahedron-shaped solid W in (u, λ, θ)-space as in Definition 2. Then by Lemma 3.1, for any point $P \in W$, the forward flow through P leaves W through the surfaces F_b, F_r, F_s, F_k. On the other hand the backward flow through P can leave W only through F_f. It is also straightforward to show that the backward layer flow cannot leave W through the six edges of W that do not form the boundary of F_f.

The projection of the u-nullsurface onto the (u, λ)-plane, the u-nullcline, divides the base rectangle $R(u_-^1, u_-^2)$ into three components: the leftmost one $\mathcal{R}_1$ above the segment of the u-nullcline that connects E_-^1 and E_+^1, the rightmost one $\mathcal{R}_3$ above the segment of the u-nullcline that connects E_+^2 and E_-^2, and the middle one $\mathcal{R}_2$ between the two segments of the u-nullcline. Define

$$V(\mathcal{R}_j) := \{(u, \lambda, \theta) : (u, \lambda) \in \mathcal{R}_j\}, \quad j = 1, 2, 3.$$

From Figures 7(a) and 7(b), $V(\mathcal{R}_2)$ is backward invariant with respect to the layer problem.

We now prove the existence of a heteroclinic solution. Note that if a heteroclinic connection exists, it has to be solely in W. The point $E_-^2 = (u_-^2, 0, 0)$ is on the supersonic branch of S_0 and is fully repelling. Thus in backward time E_-^2 is attracting all the points in a neighborhood of E_-^2. If the order of the corresponding eigenvalues is $0 < l_1 < l_2 < l_3$, then the eigenvector v_1 points along one edge of W, while the others do not point into W (see the definitions of the eigenvectors in (2.13)). On the other hand, if $0 < l_2 < l_1$, then the eigenvector v_2 points into W as well. Hence the

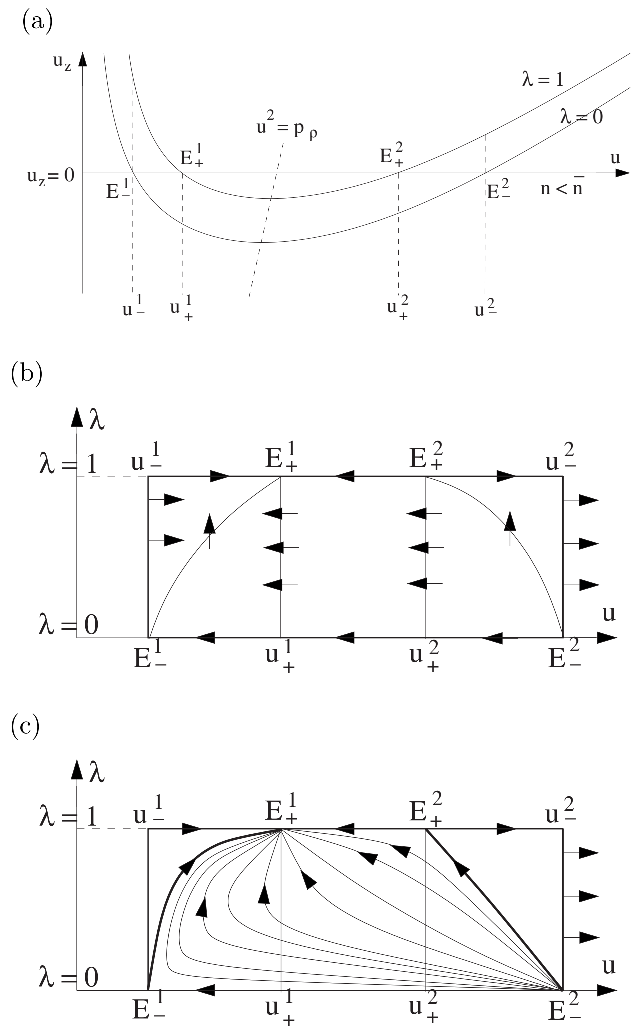

FIG. 7. (a) *shows* u_z *as a function of* (u, λ) *for a fixed* n. *The arrows in* (b) *illustrate the signs of* u_z *in the* (u, λ) *coordinates. A one-parameter family of layer solutions connecting* E_-^2 *to* E_+^1 *is plotted in* (c). *Those solutions are bounded by layer solutions* $E_-^1 \to E_+^1, E_-^2 \to E_+^2$, *the wet shock* $E_-^2 \to E_-^1$, *and the dry shock* $E_+^2 \to E_+^1$.

weakest eigendirection of E_-^2 always points into (or at least along) W.

The point $E_+^1 = (u_+, 1, 0)$ is on the subsonic branch of S_1. Thus $W^s(E_+^1)$ is two-dimensional and is spanned by the eigenvectors (v_1, v_2). The local stable manifold can be expressed as

$$W^s(E_+^1) = \{(u, \lambda, \theta) | \theta = \theta^*(u, \lambda), \|(u, \lambda)\| < \delta_0\}.$$

Consider a semicircle of radius δ in the half plane $\lambda \leq 1$ where ϕ is the angle of v measured from the negative u-axis:

$$v(\phi) = (u(\phi), \lambda(\phi)) = \delta(\cos\phi)(-1, 0) + \delta(\sin\phi)(0, -1),\ 0 \leq \phi \leq \pi. \quad (3.3)$$

Then $\{P(\phi) = (u(\phi), \lambda(\phi), \theta(\phi)) | \theta(\phi) = \theta^*(u(\phi), \lambda(\phi)),\ 0 < \phi < \pi\}$ describes a smooth arc on the local stable manifold $W^s(E_+^1)$. Its projection on the (u, λ)-plane intersects the u-nullcline at $0 < \phi = \phi_1 < \pi/2$ and the line $u = u_+^1$ at $\phi = \pi/2$. Now let ϕ_2 be the infimum of the angles such that the backward orbit through $P(\phi)$ will enter $V(\mathcal{R}_2)$. It is clear that $0 < \phi_2 < \phi_1$. For $\phi_2 < \phi < \pi$, the backward orbit through $P(\phi)$ will enter the region $V(\mathcal{R}_2)$ which is backward invariant. Since $d\lambda/dz > 0$, it follows that $\lambda(z) \to 0$ as $z \to -\infty$. The invariant set on the surface $\lambda = 0$ consists only of E_-^1 and E_-^2. Hence, the backward orbit must approach E_-^2. The forward orbit of course must approach E_+^1 so we have a layer connection $E_-^2 \to E_+^1$.

If $\phi = \phi_2$, then the backward orbit should stay above the u-nullcline and connect to E_-^1. This is a subsonic-to-subsonic layer solution and has been discussed in [14] by using the principle of Wazewski. In other words, as $\phi \to \phi_2$, the limit of the one-parameter family of $E_-^2 \to E_+^1$ layers is the union of two heteroclinic orbits: $E_-^2 \to E_-^1$ (wet shock) and $E_-^1 \to E_+^1$. Observe that not all of the supersonic-to-subsonic layers are monotone in u. The u component of some solutions can go below u_+ and then return back to u_+.

On the other hand as $\phi \to \pi$, the limit of the one-parameter family of $E_-^2 \to E_+^1$ layers is the unique pair of two heteroclinic orbits: $E_-^2 \to E_+^2$, which is a supersonic-to-supersonic connection as studied in [14], followed by the transonic layer solution E_+^2 to E_+^1 (dry shock). ∎

Corollary 3.1. *Assumption* 2 *of Theorem* 3.1 *can be weakened to*

(H1) $p < p_{eq}$ *for* $(u, \lambda) = (u_-^1, 1)$.

Proof. Note that Assumption 2 still holds within the pentahedron W since $p_\lambda > 0$ and $\partial_u p(\lambda, m/u) < 0$, which follows from $p_\rho > 0$ by Assumption 1. ∎

Making this complement to the results of Theorem 3.1, we can show the following.

Theorem 3.2. *There do not exist any subsonic-to-supersonic evaporation layer solutions connecting* $E_-^1 \in S_0$ *to* $E_+^2 \in S_1$.

Proof. This can be seen from the fact that $u_z < 0$ for $u_+^1 < u < u_+^2$. ∎

An indirect proof of Theorem 3.2 is to use a result from [14] which shows that the branch of the one-dimensional stable manifold $W^s(E_+^2)$ that stays in the pentahedron W will intersect with $W^u(E_-^2)$ and form a supersonic-to-supersonic layer solution. Therefore $W^s(E_+^2)$ will not intersect with $W^u(E_-^1)$.

3.2. Existence of sub/supersonic-to-sonic layer solutions. For $n = \bar{n}$, there are three equilibrium points $\{E_-^1, E_+, E_-^2\}$ on $S_0 \cup S_1$ marked by their u coordinates $u_-^1 < u_+ < u_-^2$. Among them $E_-^1 = (u_-^1, 0, 0) \in S_0$ is subsonic, $E_+ = (u_+, 1, 0) \in S_1$ is sonic, and $E_-^2 = (u_-^2, 0, 0) \in S_0$ is supersonic.

Theorem 3.3. *Assume* $n = \bar{n}$ *and that Assumptions* 2 *and* 3 *are satisfied with* $\bar{u} < u_-^1 < u_-^2 < \bar{\bar{u}}$. *Then there exists a one-parameter family of nonmonotone supersonic-to-sonic heteroclinic solutions to the layer problem* (2.4) *connecting* E_-^2 *to* E_+ *(see Figure* 8*). Every solution in that family approaches* E_+ *by being tangent to the part of the u-axis where* $u < u_+$.

There is also a unique subsonic-to-sonic layer $E_-^1 \to E_+$. *Together with the layer solution* $E_-^2 \to E_-^1$ *along the line* $\lambda = 0$ *(wet shock), this pair of heteroclinic solutions is a boundary of the one-parameter family of* $E_-^2 \to E_+$ *layer solutions.*

The other boundary of that one-parameter family of $E_-^2 \to E_+$ *layer solutions is a unique monotone supersonic-to-sonic layer solution* $E_-^2 \to E_+$ *that approaches* E_+ *by being tangent to the part of* $W^s(E_+)$ *where* $\lambda < 1$.

Proof. Consider a pentahedron shaped solid W in (u, λ, θ)-space based on the rectangle $R(u_-^1, u_-^2)$ as in Definition 2. Then by Lemma 3.1, for any point $P \in W$, the forward flow through P leaves W through the surfaces F_b, F_r, F_s, F_k. On the other hand the backward flow through P can leave W only through F_f. It is also

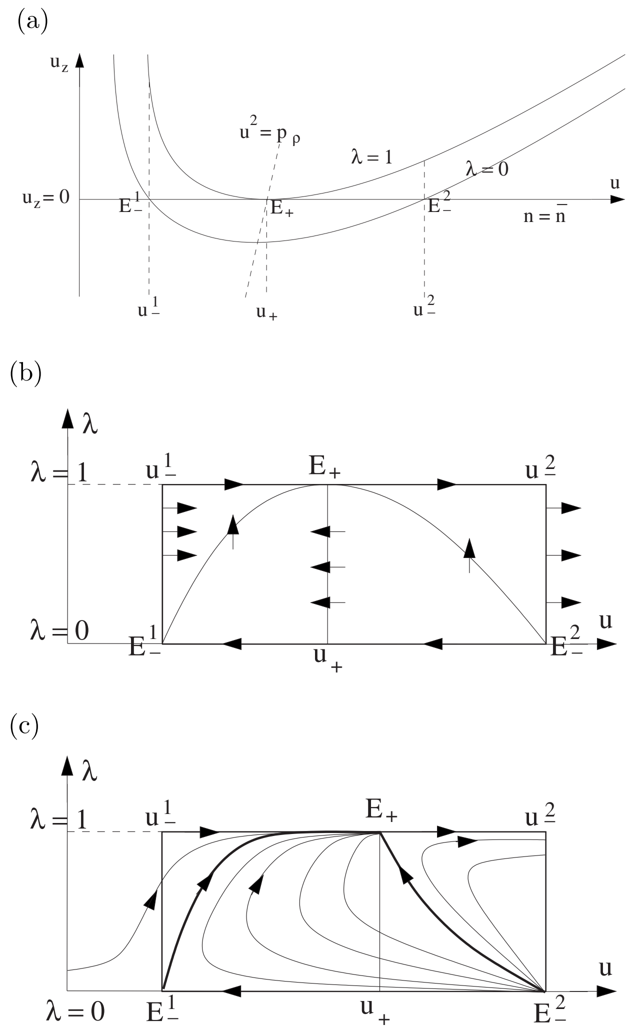

Fig. 8. (a) *shows* u_z *as a function of* (u, λ) *for a fixed* $n = \bar{n}$. *The arrows in* (b) *illustrate the signs of* u_z *in the* (u, λ) *coordinates. A one-dimensional family of layer solutions connecting* E^2_- *to* E_+ *is plotted in* (c). *Those solutions are bounded by layer solutions* $E^1_- \to E_+, E^2_- \to E_+$ *and the wet shock* $E^2_- \to E^1_-$.

straightforward to show that the backward layer flow cannot leave W through the six edges of W that do not form the boundary of F_f.

The u-nullcline divides the base rectangle $R(u^1_-, u^2_-)$ into three components: the leftmost one $\mathcal{R}_1$ above the segment of the u-nullcline that connects E^1_- and E_+, the middle one $\mathcal{R}_2$ below the u-nullcline, and the rightmost one $\mathcal{R}_3$ above the segment of the u-nullcline that connects E^2_- and E_+. Note that $V(\mathcal{R}_2)$ is backward invariant under the flow of the layer problem.

The equilibrium point $E^2_- = (u^2_-, 0, 0)$ on the supersonic branch of S_0 is an unstable node. The equilibrium point $E^1_- = (u^1_-, 0, 0)$ on the subsonic branch of S_0 has a two-dimensional unstable manifold $W^u(E^1_-)$. The corresponding unstable eigenspace is spanned by the eigenvectors $\{v_2, v_3\}$. Only the eigenvector v_2 corresponding to the weaker unstable eigenvalue points into W (we have $l_1 < 0 < l_2 < l_3$); see the definitions of eigenvectors in (2.13). This already guarantees that part of the (local) manifold $W^u(E_-)$ lies within the pentahedron W.

The point $E_+ = (u_+, 1, 0)$ on the sonic surface of S_1 has a two-dimensional center-stable manifold $W^{cs}(E_+)$. The corresponding center-stable eigenspace is spanned by the eigenvectors $\{v_1, v_2\}$ (we have $l_2 < l_1 = 0 < l_3$); see the definitions of eigenvectors in (2.13). The eigenvector v_1 points along an edge of W, while the eigenvector $-v_2$ points into W. The signs of the components of $-v_2$ are $(+, -, +)$; therefore there is a branch of the stable manifold $W^s(E_+)$ that enters the region $V(\mathcal{R}_2)$ which is invariant with respect to the backward flow. The backward flow of that branch of $W^s(E_+)$ will remain in $V(\mathcal{R}_2)$ and its α-limit set is the point E_-^2. This proves the existence of a unique layer connection $E_-^2 \to E_+$ that approaches E_+ exponentially fast and is monotone in u.

The local center-stable manifold of $W^{cs}(E_+)$ can be expressed as

$$W^{cs}(E_+) = \{(u, \lambda, \theta) | \theta = \theta^*(u, \lambda), \|(u, \lambda)\| < \delta_0\}.$$

Note that $W^c(E_+)$ is semistable: it is stable from the side $u < u_+$ and is unstable from the side $u > u_+$. The center-stable manifold $W^{cs}(E_+)$ is divided by $W^s(E_+)$ into two components; call them the stable and unstable parts of $W^{cs}(E_+)$. An orbit on $W^{cs}(E_+) \backslash W^s(E_+)$ must follow the stable fibers of the foliation of $W^{cs}(E_+)$ and, hence, approaches $W^c(E_+)$ exponentially. On the other hand, the motion of the projection of such an orbit along the stable fibers on $W^c(E_+)$ is only algebraic (nonexponential). If the projection of such an orbit along the stable fibers is on the stable part of $W^{cs}(E_+)$, then it will approach E_+ nonexponentially and tangent to the branch of $W^c(E_+)$ that is below u_+. If it is on the unstable part of $W^{cs}(E_+)$, then it will leave E_+ following the flow of the unstable branch of $W^c(E_+)$ where $u > u_+$.

To study these two possibilities, define the semicircle on $W^{cs}(E_+)$ as in (3.3). Then $P(\phi) := \{(u(\phi), \lambda(\phi), \theta(\phi)),\ 0 \le \phi \le \pi\}$ is a smooth arc on $W^{cs}(E_+)$. Its projection to the (u, λ)-plane intersects the subsonic part of the u-nullcline at $\phi = \phi_2$ and the projection of $W^s(E_+)$ at $\phi = \phi_3$. Let ϕ_1 be the infimum of all the angles ϕ such that the backward orbit through $P(\phi)$ will enter the region $V(\mathcal{R}_2)$. Note that $0 < \phi_1 < \phi_2 < \pi/2 < \phi_3 < \pi$.

If $\phi_1 < \phi < \pi$, then the orbit passing through $P(\phi)$ approaches E_-^2 in backward time due to the facts that the region $V(\mathcal{R}_2)$ is backward invariant and the (λ, u) components in $V(\mathcal{R}_2)$ are monotone. Consider the ω-limit set of an orbit through $P(\phi)$. If $\phi < \phi_3$, then the ω-limit set of the orbit through $P(\phi)$ is E_+, while if $\phi > \phi_3$, the ω-limit set does not exist since the orbit leaves W through the side F_k and is unbounded. This shows that if $\phi_1 < \phi < \phi_3$, the one-dimensional family of supersonic-to-sonic connection $E_-^2 \to E_+$ exists. Each orbit in that family is not monotone in u and does not approach E_+ exponentially. As $\phi \to \phi_3$, the limit of the one-parameter family of supersonic-to-subsonic layer is the unique $E_-^2 \to E_+$ connection that passes through $P(\phi_3)$. It is monotone in u and approaches E_+ exponentially along the stable manifold $W^s(E_+)$.

We now show that the orbit through $P(\phi_1)$ is a connection $E_-^1 \to E_+$. For any $\kappa > 0$, there exist $\phi_1^{\pm}$ such that $|\phi_1^{\pm} - \phi_1| < \kappa$, $\phi_1^- < \phi_1 < \phi_1^+$, and the backward orbit through $P(\phi_1^-)$ leaves $V(\mathcal{R}_1)$ through the surface F_f, and the backward orbit through $P(\phi_1^+)$ leaves $V(\mathcal{R}_1)$ through the surface whose projection to the (u, λ)-plane is the u-nullcline to $V(\mathcal{R}_2)$. By the principle of Wazewski, there exists a $\phi_0 \in (\phi_1^-, \phi_1^+)$ such that the orbit through $P(\phi_0)$ remains in $V(\mathcal{R}_1)$ in backward time. Hence it

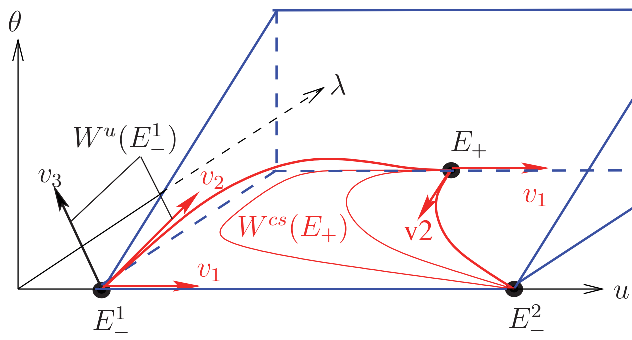

FIG. 9. *The unique subsonic-to-sonic heteroclinic connection $E_-^1 \to E_+$ corresponds to a transverse intersection of the manifolds $W^{cs}(E_+)$ and $W^u(E_-^1)$ within the pentahedron W.*

approaches E_-^1 in backward time. Since $|\phi_0 - \phi_1|$ can be arbitrarily small, the orbit through $P(\phi_1)$ should also approach E_-^1 in backward time. The ω-limit point of this orbit is E_+ due to the fact $0 < \phi_1 < \phi_3$.

We have shown that the one-parameter family of supersonic-to-sonic layer $E_-^2 \to E_+$ has a limit as $\phi \to \phi_1$. The limit consists of a pair of heteroclinic orbits, $E_-^2 \to E_-^1$ (wet shock), followed by a subsonic-to-sonic layer solution, $E_-^1 \to E_+$.

Finally, note that $\dim(W^u(E_-^2) \cap W^{cs}(E_+)) = 2$, i.e., $W^{cs}(E_+)$ has a full intersection with $W^u(E_-^2)$. Furthermore, $\dim(W^u(E_-^2) \cap W^s(E_-^1)) = 1$, i.e., $W^s(E_-^1)$ has a full intersection with $W^u(E_-^2)$. Since we showed that the pair of heteroclinic orbits, $E_-^2 \to E_-^1$ and $E_-^1 \to E_+$, is part of the boundary of the two-dimensional manifold $W^u(E_-^2) \cap W^{cs}(E_+)$, it follows that the tangent space of the two-dimensional manifold $W^{cs}(E_+)$ is locally spanned near E_-^1 by its stable eigenvector v_1 and the weak stable eigenvector v_2. Observe that the strong unstable eigenvector v_3 is transverse to the tangent space spanned by $\{v_1, v_2\}$. Thus $TW^u(E_-^1) + TW^{cs}(E_+)$ is three-dimensional near E_-^1. This shows that the intersection of these manifolds is transverse and the subsonic-to-sonic layer $E_-^1 \to E_+$ is unique (see Figure 9). ☐

Similar to Corollary 3.1, we have the following.

COROLLARY 3.2. *Assumption* 2 *of Theorem* 3.3 *can be weakened to*
(H1) $p < p_{eq}$ *for* $(u, \lambda) = (u_-^1, 1)$.

4. Analysis of the reduced (outer) problem on slow manifolds. The phase space of the reduced system (2.5) is the critical manifold S (2.8). We only focus on the reduced flow on S_0 and S_1 since S_e does not play a role in our analysis of evaporation waves (Assumption 2).

PROPOSITION 4.1. *The reduced vector field on S_0 and S_1 points away from the sonic fold surface $u^2 = p_\rho$.*

Proof. Since S_0 and S_1 are given as graphs over (r, m, u)-space, we study the reduced flow in this single (r, m, u)-chart. Hence, we differentiate $n = N(m, u)$ with respect to the slow scale y to obtain the reduced system (2.5) in the (r, m, u)-chart

$$
\begin{aligned}
r_y &= 1, \\
m_y &= -\frac{2m}{r}, \\
N_u u_y &= \frac{2mu}{r} + N_m \frac{2m}{r}\,.
\end{aligned}
\tag{4.1}
$$

Since $n = N(m,u) = -mu - p(\Lambda(m,u), \frac{m}{u})$, we have $N_u = -m - p_\lambda \Lambda_u - p_\rho \rho_u$ and $N_m = -u - p_\lambda \Lambda_m - p_\rho \rho_m$. The derivatives of the function Λ evaluated on S_0, respectively, S_1, are $\Lambda_m = \Lambda_u = 0$. Using $\rho = m/u$ to evaluate ρ_u and ρ_m, we obtain the reduced system on S_0, respectively, S_1:

$$\begin{aligned} r_y &= 1, \\ m_y &= -\frac{2m}{r}, \\ (u^2 - p_\rho) u_y &= \frac{2u}{r} p_\rho \,. \end{aligned} \tag{4.2}$$

Note that this system is singular along the sonic surface defined by $u^2 = p_\rho$. We desingularize the system by the rescaling $dy = (u^2 - p_\rho) d\bar{y}$, which gives the *desingularized system*

$$\begin{aligned} r_{\bar{y}} &= (u^2 - p_\rho), \\ m_{\bar{y}} &= -\frac{2m}{r}(u^2 - p_\rho), \\ u_{\bar{y}} &= \frac{2u}{r} p_\rho > 0 \,. \end{aligned} \tag{4.3}$$

The phase portraits of the reduced and desingularized system are equivalent up to a change of orientation in the subsonic domain, i.e., $u^2 < p_\rho$. Hence $u_y < 0$ in the subsonic domain and $u_y > 0$ in the supersonic domain, which implies that the reduced flow moves away from the sonic fold surface $u^2 = p_\rho$ on S_0, respectively, S_1. Note that this follows because the sonic surface is given as a graph $u = U(m)$ for $m > 0$ independent of r (see also Proposition 5.1). Since we assume $u > 0$, this also implies that there exists no ordinary or folded singularities on S_0 or S_1. ∎

Remark 4.1. Observe that S_0 and S_1 represent manifolds of equilibria for the layer problem (2.4). The part of S_0 and S_1 that satisfies $u^2 \neq p_\rho$ consists of hyperbolic equilibrium points of the first three equations of the layer problem. Thus, on S_0 or S_1, if $u^2 \neq p_\rho$, u can be solved as a function of (m, n, r) and has two smooth branches. One is subsonic and the other is supersonic according to the signs of $u^2 - p_\rho$. If we use $d = u^2 - p_\rho$ to measure the distance to the sonic surface, it is shown in [14] that when restricted to the super- or subsonic branch of $S_0 \cup S_1$, $(d^2)_y > 0$ with respect to the reduced problem (2.5). Therefore, a solution staying on the critical manifold S_0 (or S_1) will not correspond to a transonic wave.

5. Existence of transonic evaporation waves for $0 < \varepsilon \ll 1$. From Proposition 4.1 it follows that a transonic evaporation wave must have an internal layer at some $r = r_i \in (r_0, r_1)$, as shown in Figure 2. To form a singular standing wave profile Γ for $r \in [r_0, r_1]$ such an internal layer solution γ_i has to be concatenated with two (outer) solutions from the reduced problem, one on the subsonic (supersonic) branch of S_0 for $r \in [r_0, r_i]$ denoted by γ_0, and the other on the supersonic (subsonic) branch of S_1 for $r \in [r_i, r_1]$ denoted by γ_1. In the following, we show the existence of (nondegenerate) transonic evaporation waves for $0 < \varepsilon \ll 1$ that exist near a singular ($\varepsilon = 0$) wave profile $\Gamma = \gamma_0 \cup \gamma_i \cup \gamma_1$ (see Figure 3) in the supersonic-to-subsonic case (section 5.1) and the subsonic-to-supersonic case (section 5.2).

The sub- and supersonic branches of S_0 (respectively, S_1) away from the sonic surface are normally hyperbolic, with three zero eigenvalues whose eigenspace is tangent to S_0 (respectively, S_1). Fenichel's theory [16] implies that these normally hyperbolic manifolds perturb smoothly to $O(\varepsilon)$-close slow manifolds $S_0(\epsilon)$ (respectively, $S_1(\epsilon)$), and the slow flow on these manifolds is an $O(\varepsilon)$ smooth perturbation of the corresponding reduced flow. In the same manner, the end points P_0 and P_1 of Γ perturb smoothly to $P_0(\epsilon)$ and $P_1(\epsilon)$, respectively.

Remark 5.1. It is well known that the slow manifolds $S_0(\epsilon)$, respectively, $S_1(\epsilon)$, are not unique but they represent a family of slow manifolds that lie within $O(\exp(-K/\varepsilon))$ distance from each other for some $K > 0$. We make an arbitrary choice of $S_0(\epsilon)$, respectively, $S_1(\epsilon)$, and show that the results obtained in this section are independent of such a choice.

5.1. Supersonic-to-subsonic evaporation waves. Assume that an internal layer solution γ_i from Theorem 3.1 is given which connects the three-dimensional manifold $W^u(E_-^2)$ on the supersonic region of S_0, denoted by S_0^{super}, to the two-dimensional manifold $W^s(E_+^1)$ on the subsonic region of S_1, denoted by S_1^{sub} (see Figure 7). To construct the concatenated orbit Γ, we must find γ_1 as a forward orbit from E_+^1 and γ_0 as a backward orbit from E_-^2. The existence of such a solution γ_1 that stays on the subsonic region S_1^{sub} is guaranteed since the reduced flow of (4.2) moves away from the sonic fold. We assume that γ_1 forward connects E_+^1 to P_1 at $r = r_1$. On the other hand, the backward solution γ_0 on S_0^{super} with initial condition given by E_-^2 might reach the sonic fold for some $r \in (r_0, r_i)$. To avoid this, the following assumption will be used.

Assumption 4. The distance $|r_i - r_0|$ is sufficiently small such that the backward solution γ_0 of the reduced problem (4.2) starting at $r = r_i$ with initial condition $E_-^2 \in S_0^{super}$ given by the internal layer γ_i stays in the supersonic region S_0^{super} for all $r \in [r_0, r_i]$.

By Assumption 4, we assume γ_0 backward connects E_-^2 to P_0 at $r = r_0$ following the reduced flow on S_0^{super}.

THEOREM 5.1. *Under Assumptions* 1–4, *let* $\Gamma = \gamma_0 \cup \gamma_i \cup \gamma_1$ *denote a singular evaporation wave in the phase space of system* (2.3) *which is a concatenation of an internal layer solution* γ_i *of* (2.4) *at* $r = r_i$ *connecting the supersonic branch* S_0^{super} *with the subsonic branch* S_1^{sub}*, an outer solution* γ_0 *of the reduced problem* (2.5) *on the supersonic branch* S_0^{super} *for* $r \in [r_0, r_i]$*, and another outer solution* γ_1 *of the reduced problem* (2.5) *on the subsonic branch* S_1^{sub} *for* $r \in [r_i, r_1]$*.*

If $\varepsilon_0 > 0$ *is sufficiently small, then for all* $\varepsilon \in (0, \varepsilon_0)$ *there exists a two-dimensional family of standing wave solutions* $\Gamma(\epsilon)$ *of system* (2.3) *lying within* $O(\epsilon)$ *of* Γ*.*

Proof. The normally hyperbolic supersonic branch S_0^{super} has an associated local unstable manifold $W^u(S_0^{super}) = \bigcup_{p_0 \in S_0^{super}} W^u(p_0)$ (unstable layer fibration) and the normally hyperbolic subsonic branch S_1^{sub} has an associated local stable manifold $W^s(S_1^{sub}) = \bigcup_{p_1 \in S_1^{sub}} W^s(p_1)$ (stable layer fibration). Fenichel's theory [16] implies that these local unstable and stable manifolds (fibrations) $W^u(S_0^{super})$ and $W^s(S_1^{sub})$ perturb smoothly to $O(\varepsilon)$-close local unstable and stable manifolds (fibrations) $W^u(S_0^{super}(\varepsilon))$ and $W^s(S_1^{sub}(\varepsilon))$.

Observe that the two projections of the outer solutions γ_j, $j = 0, 1$, of Γ onto the slow variable space (m, n, r) intersect at the common $n(r_i)$, which is the n-coordinate for E_-^2 and E_+^1. From the third equation of (2.5) it is easily proved that the two (projected) solutions intersect transversely. Thus for $0 < \varepsilon \ll 1$, the two (projected) solutions intersect transversely $O(\varepsilon)$ nearby, i.e., at the common n-coordinate $n^\varepsilon = n(r_i^\epsilon = r_i + O(\varepsilon))$, and we denote the corresponding common points by $E_-^2(\epsilon)$ and $E_+^1(\epsilon)$. The outer trajectory $\gamma_0 \in S_0^{super}$, connecting E_-^2 to P_0, perturbs $O(\varepsilon)$ smoothly to the trajectory $\gamma_0(\varepsilon) \in S_0^{super}(\varepsilon)$, connecting $E_-^2(\varepsilon)$ to $P_0(\varepsilon)$, while $\gamma_1 \in S_1^{sub}$, connecting E_+^1 to P_1, perturbs $O(\varepsilon)$ smoothly to the trajectory $\gamma_1(\varepsilon) \in S_1^{sub}(\varepsilon)$, connecting $E_+^1(\varepsilon)$ to $P_1(\varepsilon)$.

In Theorem 3.1 we have shown that there exists a supersonic-to-subsonic evaporation layer solution γ_i connecting base points $E_-^2 \in S_0^{super}$ and $E_+^1 \in S_1^{sub}$. Since this layer fiber intersection of $W^u(E_-^2) \subset W^u(S_0^{super})$ and $W^s(E_+^1) \subset W^s(S_1^{sub})$ is transverse and the projection of $\gamma_0(\varepsilon)$ and $\gamma_1(\varepsilon)$ onto the slow variable space is transverse at the common base points $E_-^2(\epsilon)$ and $E_+^1(\epsilon)$, this fiber intersection will persist for $0 < \epsilon \ll 1$, i.e., the unstable fibers $W^u(E_-^2(\epsilon))$ transversely intersect with the stable fibers $W^s(E_+^1(\epsilon))$. Thus $W^u(E_-^2(\varepsilon)) \cap W^s(E_+^1(\varepsilon))$ is a two-dimensional submanifold.

For each point ζ on the two-dimensional intersection surface $W^u(E_-^2(\varepsilon)) \cap W^s(E_+^1(\varepsilon))$, we construct an orbit $\Gamma(\varepsilon)$ which exponentially approaches $S_0^{super}(\varepsilon)$ in backward time along its unstable fibers and exponentially approaches $S_1^{sub}(\varepsilon)$ in forward time along its stable fibers. Since the unstable fibers of $S_0^{sub}(\varepsilon)$ are backward invariant with respect to the flow, $\Gamma(\varepsilon)$ is on the unstable fibers of $P_0(\varepsilon)$ at $r = r_0$. Also the stable fibers are forward invariant to the flow. Thus $\Gamma(\varepsilon)$ is on the stable fibers of $P_1(\varepsilon)$ at $r = r_1$. Let the solution that passes through ζ at $r = r_i^\epsilon$ be denoted by $q(r, \zeta, \varepsilon)$.[1] Then $q(r_0, \zeta, \varepsilon) = (m, n, u, \lambda, \theta)(r_0)$ is exponentially close to $P_0(\epsilon)$ and is in the supersonic region with $\lambda(r_0) \approx 0$. Also $q(r_1, \zeta, \varepsilon) = (m, n, u, \lambda, \theta)(r_1)$ is exponentially close to $P_1(\varepsilon)$ and is in the subsonic region with $\lambda(r_1) \approx 1$. Thus $q(r, \zeta, \varepsilon)$, whose orbit is $\Gamma(\varepsilon)$, is a supersonic-to-subsonic evaporation wave. Such waves form a two-dimensional family determined by the choice of ζ.

As mentioned in Remark 5.1, the solution $\Gamma(\epsilon)$ is unique once the choices $S_0^{super}(\epsilon)$ and $S_1^{sub}(\epsilon)$ have been made, and the differences due to choices are only exponentially small. ∎

5.1.1. Boundary conditions that determine a unique supersonic-to-subsonic wave. Theorem 5.1 proved the existence of a two-dimensional family of supersonic-to-subsonic evaporation waves, but it does not address the uniqueness of these waves. In the following we prescribe boundary conditions at $r = r_0$ and $r = r_1$ to obtain a unique transonic evaporation wave. The boundary condition shall be given by two boundary manifolds $B_j, j = 0, 1$:

$$(r, m, n, u, \lambda, \theta)(r_j) \in B_j, \quad j = 0, 1.$$

For simplicity, we assume that B_0 and B_1 are linear affine planes that are defined by splitting the conditions on slow and fast variables. First, we define the following "slow" submanifolds $B_j^s, j = 0, 1$.

Assumption 5. For the slow variables $(r, m, n) \in B_j^s$, either $n(r_0) = n_0$ or $n(r_1) = n_1$ is given. Also, either $m(r_0) = m_0$ or $m(r_1) = m_1$ is given.

The conditions given in Assumption 5 provide four choices of putting constraints on the slow part B_j^s of the boundary manifolds B_j, $j = 0, 1$. There is an obvious constraint on the variable r, that is, at $y = r_0, r(r_0) = r_0$. Using, $dr/dy = 1$, at the other end of the boundary we will have $r(r_1) = r_1$. Altogether we have introduced three conditions on the slow variables (m, n, r).

For $\epsilon = 0$, we assume an internal layer at $r = r_i$. Thus for a given layer position $r = r_i$ and for boundary conditions on (m, n) given by Assumption 5, the end points $\{P_0, P_1, E_-^2, E_+^1\}$ of the segments of the singular orbit $\Gamma = \gamma_0 \cup \gamma_i \cup \gamma_1$ defined in Theorem 5.1 are uniquely determined.

[1] Note that since $y = r$, and $z = r/\varepsilon$, we write solutions as functions of r.

For the fast variables (u, λ, θ), we define the following "fast" submanifolds $B_j^f, j = 0, 1$.

Assumption 6. The manifold B_0^f is one-dimensional and is transverse to the weakest two unstable eigenspaces of P_0, spanned by $\{\mathbf{v}_1, \mathbf{v}_2\}$. The manifold B_1^f is two-dimensional and is transverse to the local unstable manifold of P_1.

DEFINITION 3 (boundary manifolds, super to sub). *Under Assumptions* 5–6*, let $B_0^* = B_0^s \times B_0^f$ and $B_1^* = B_1^s \times B_1^f$ be the product of slow and fast planes. The boundary manifolds are given by $B_0 = B_0^* + q(r_0, \zeta, \varepsilon)$, $\zeta \in W^u(E_-^2(\varepsilon)) \cap W^s(E_+^1(\varepsilon))$, and $B_1 = B_1^* + Q_1$, where Q_1 is any point near P_1.*

Remark 5.2. In a typical linear PDE, the boundary conditions are given first, and then the existence of solutions is proved. If we assign boundary conditions without any foreknowledge of the solutions of the nonlinear problem, the solution of the BVP may not exist. So our boundary conditions are based on the knowledge of the singular limit solution of the transonic waves.

Note that B_0 depends on the prescribed ϵ, while B_1 is independent of ϵ. If B_1 happens to pass through $q(r_1, \zeta, \epsilon)$, then $q(r, \zeta, \epsilon)$ obviously satisfies the boundary conditions defined by B_0 and B_1 (and is the unique such solution). However, we do not want to define the boundary manifolds to pass the end points of the standing wave, then claim that a solution exists. We want the boundary condition to have some room for error, and the solution should be robust with respect to perturbations of the boundary conditions. From the application point of view, it is important that one can maintain physical conditions at both ends of the nozzle with some error and still have a solution. This explains why we assume that Q_1 is close to but not equal to P_1.

Recall that for the supersonic branch S_0^{super}, the eigenvalues for the fast system with $(m, n, r) \in S_0$ satisfy the condition $0 < \ell_1,\ 0 < \ell_2 < \ell_3$. The following assumption shall be used in the next theorem.

Assumption 7. For the singular wave γ_0 on S_0^{super} defined from $r = r_0$ to $r = r_i$, the eigenvalues for the fast system where $(m, n, r) \in \gamma_0$ satisfy $\ell_1 < \ell_3$, i.e., ℓ_3 is the strongest unstable eigenvalue.

THEOREM 5.2. *Let $q(r, \zeta, \epsilon)$ be a family of evaporation waves that passes the initial value $\zeta \in W^u(E_-^2(\varepsilon)) \cap W^s(E_+^1(\varepsilon))$ at $r = r_i^\epsilon = r_i + O(\epsilon)$. Assume that the family of solutions is tangent to the two weaker unstable fibers based at $P_0(\epsilon)$ and that Assumption* 7 *is satisfied. Then the boundary manifolds B_0 and B_1 given by Definition* 3 *determine a unique supersonic-to-subsonic evaporation wave.*

Proof. The standing wave that satisfies the boundary conditions (Definition 3) can be expressed as

$$U(r, \epsilon) := \Phi(r - r_0, \varepsilon)B_0 \cap \Phi(r - r_1, \varepsilon)B_1, \quad r_0 \le r \le r_1. \tag{5.1}$$

It suffices to show that for one particular r, the intersection defined by the right-hand side of (5.1) is a unique nonempty point. To this end, we shall use Fenichel theory on the persistence of hyperbolic part of the slow manifolds and their fibrations (or foliations).

Fenichel theory implies for sufficiently small $0 < \varepsilon \ll 1$ that B_0 transversely intersects the "fast" subspace spanned by the two weakest unstable fiber directions of $P_0(\epsilon)$ as well as B_1 transversely intersects the unstable fiber of $P_1(\epsilon)$.

First, we focus on the intersection of the slow components of B_0 and B_1 projected onto the slow variable space. Under Assumption 5, the singular limit segments γ_j, $j = 0, 1$, of Γ are uniquely determined.

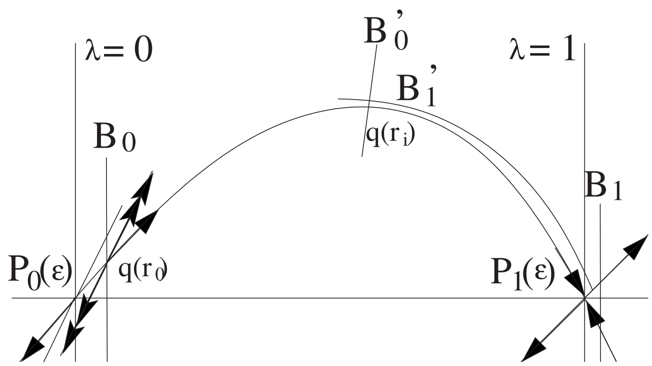

FIG. 10. *Only the fast variables are plotted. The forward image of the manifold B_0 is B_0', while the backward image of the manifold B_1 is B_1'. At $r = r_i^\varepsilon$, these manifolds intersect transversely.*

As shown in the proof of Theorem 5.1, the two projections of γ_j, $j = 0, 1$, onto the slow variable space (m, n, r) intersect transversely at the common $n(r_i)$. Thus for $0 < \varepsilon \ll 1$, the two (projected) solutions intersect transversely $O(\varepsilon)$ nearby, i.e., at the common n-coordinate $n^\varepsilon = n(r_i^\varepsilon)$, and, as before, we denote the corresponding common points by $E_-^2(\epsilon)$ and $E_+^1(\epsilon)$.

Next, we shall use the theorem of graph transformation to complete the proof. When the flow is near a saddle equilibrium point, such a theorem is called the *lambda lemma*, or *inclination lemma*. In singular perturbed systems, such a theorem is also called the *exchange lemma* [19]. Let $\Phi(y, \varepsilon)$ denote the flow of the nonlinear system (2.2) for $\varepsilon > 0$. Since B_1 transversely intersects the unstable fiber $W^u(P_1(\epsilon))$, the backward image $B_1' = \Phi(r_i^\varepsilon - r_1, \varepsilon)B_1$ is C^1 close to the stable fibers at $E_+^1(\epsilon)$.

On the other hand, since the unstable fibers of $P_0(\varepsilon)$ are three-dimensional, the regular lambda lemma or exchange lemma does not apply. A *generalized lambda lemma* was proved in [25] which can be extended to apply to this case. Recall that $E_-^2(\epsilon) = \Phi(r_i^\varepsilon - r_0, \epsilon)P_0(\epsilon)$. From Assumption 7, the eigenvalues for the fast system do not change order following the slow flow from $P_0(\varepsilon)$ to $E_-^2(\epsilon)$. Therefore the generalized lambda lemma should also apply to our fast system. Since B_0 is transverse to the two weakest eigenvectors of $P_0(\epsilon)$, its forward image under the flow, $B_0' = \Phi(r_i^\varepsilon - r_0, \varepsilon)B_0$ is C^1 close to the strongest unstable fiber of $E_-^2(\epsilon)$. In particular, B_0' is transverse to the two weakest unstable fibers based at $E_-^2(\varepsilon)$, which is the same as the two-dimensional stable fiber space based at $E_+^1(\epsilon)$, as assumed in this theorem. The fact that B_1' is C^1 close to the stable fibers at $E_+^1(\epsilon)$ ensures the transverse intersection of B_0' and B_1' at $r = r_i^\epsilon$.

Finally, at $r = r_i^\varepsilon$, the transverse intersection of $\Phi(r_i^\varepsilon - r_0, \varepsilon)B_0 \cap \Phi(r_i^\varepsilon - r_1, \varepsilon)B_1$, at a unique point near ζ determines the evaporation wave solution that satisfies the boundary values defined by B_0 and B_1 at r_0 and r_1, respectively. This is illustrated in Figure 10.

Note that due to the transverse intersection $\Phi(r_i^\varepsilon - r_0, \varepsilon)B_0 \cap \Phi(r_i^\varepsilon - r_1, \varepsilon)B_1$, the existence and uniqueness of the transonic evaporation wave $U(r, \epsilon)$ is independent of the choice of $S_0^{super}(\epsilon)$ or $S_1^{sub}(\epsilon)$, as seen from definition (5.1) and as mentioned in Remark 5.1. □

Remark 5.3. The heteroclinic orbits in the fast system are connections from node to saddle equilibrium points, similar to the waves in KPP/Fisher equations. Based on the observation made in [25], it is necessary to assume that B_0 passes through $q(r_0, \zeta, \epsilon)$ for some $\zeta \in W^u(E_-^2(\varepsilon)) \cap W^s(E_+^1(\varepsilon))$. In fact, if the initial manifold $B_0 \cap W^u(P_0(\epsilon))$ does not intersect with the family of waves $q(r, \zeta, \epsilon)$ under consideration, then the boundary value problem does not have a solution near such waves. The reason is simply because the weakest unstable fibers are unstable in the three-dimensional unstable fiber space of $P_0(\epsilon)$. Any point on $B_0 \cap W^u(P_0(\varepsilon))$ that is not on the weakest unstable fiber gets pushed further away if $r > r_0$, so it will never be a boundary manifold for any evaporation wave that stays near $q(r, \zeta, \epsilon)$. See [25] for a proof of this on the node-to-saddle waves in KPP/Fisher-type equations, which is similar to our system.

We also remark that Assumption 7 used in Theorem 5.2 is not the most general one. As long as the eigenvalues for the fast system do not change order along γ_0, the conclusion of the theorem still holds.

Remark 5.4. Note that if Q_1 happens to be P_1, then as $\epsilon \to 0$, the solution satisfying the boundary conditions will approach Γ, which has P_1 as its right end point at $r = r_1$. On the other hand, if Q_1 is near P_1, and the tangent plane of B_1 is specified, the boundary surface will intersect the unstable fiber of P_1 at a unique point Q_1'. As $\epsilon \to 0$, the wave solution will approach the union of Γ and part of the unstable manifold connecting P_1 to Q_1'. Such boundary layer–like behavior has been discussed in [25] if the solution has a node-to-saddle-type internal layer, and in [24] if the solution has a saddle-to-saddle-type internal layer. General boundary conditions for singularly perturbed slow-fast system are that B_1 must intersect transversely with the unstable fibers that pass through P_1; see [24]. We did not assume that Q_1 in Definition 3 is on the unstable fiber of P_1, so the construction of B_1 does not require the precise knowledge of the unstable fiber of P_1.

5.2. Subsonic-to-supersonic evaporation waves. This section is dedicated to subsonic-to-supersonic evaporation waves for $0 < \varepsilon \ll 1$. Although there exists no subsonic-to-supersonic evaporation layer solution (Theorem 3.2), we are still able to construct a singular ($\varepsilon = 0$) subsonic-to-supersonic evaporation wave profile $\Gamma^s = \gamma_0 \cup \gamma_i \cup \gamma_1$ by concatenation of the (unique) critical internal layer solution γ_i from Theorem 3.3, which connects the base point E_-^1 on the subsonic region S_0^{sub} to the base point E_+ on the sonic region S_1^{super} (see Figure 8), and outer solutions γ_0 on the subsonic branch S_0^{sub} and γ_1 on the supersonic branch S_1^{super} starting on the sonic fold. The existence of such a supersonic γ_1 that stays on S_1^{super} is always guaranteed. However, to ensure the existence of a subsonic γ_0 that stays on S_0^{sub} until it reaches $r = r_0$, we need Assumption 4, as stated before Theorem 5.1 adapted to the subsonic case.

Assumption 8. The distance $|r_i - r_0|$ is sufficiently small such that the backward solution γ_0 of the reduced problem (4.2) starting at $r = r_i$ with initial condition $E_-^1 \in S_0^{sub}$ given by the internal layer γ_i stays in the subsonic region S_0^{sub} for all $r \in [r_0, r_i]$.

As in section 5.1.1, we prescribe boundary conditions at $r = r_0$ and $r = r_1$ via boundary manifolds B_j, $j = 0, 1$, to obtain a unique transonic evaporation wave. Again for simplicity, we assume that B_0 and B_1 are linear affine planes that are defined by splitting the conditions on slow and fast variables. The "slow" submanifolds B_j^s, $j = 0, 1$, are defined as in Assumption 5. For the fast variables (u, λ, θ), we define the following "fast" submanifolds B_j^f, $j = 0, 1$.

Assumption 9. The manifold B_0^f is two-dimensional and is transverse to the local stable manifold $W^s(P_0)$. The manifold B_1^f is one-dimensional and is transverse to the local unstable manifold $W^u(P_1)$.

DEFINITION 4 (boundary manifolds, sub to super). *Under Assumptions* 5 *and* 9, *let* $B_0^* = B_0^s \times B_0^f$ *and* $B_1^* = B_1^s \times B_1^f$ *be the product of slow and fast planes. The boundary manifolds are given by* $B_0 = B_0^* + Q_0$ *and* $B_1 = B_1^* + Q_1$, *where* Q_0 *is any point near* P_0 *and* Q_1 *is any point near* P_1.

THEOREM 5.3. *Under Assumptions* 1, 2, 3, *and* 8, *let* $\Gamma^s = \gamma_0 \cup \gamma_i \cup \gamma_1$ *denote a singular evaporation wave in the phase space of system* (2.3), *which is a concatenation of an internal layer solution* γ_i *of* (2.4) *at* $r = r_i$ *connecting the subsonic branch* S_0^{sub} *with the sonic fold of* S_1, *an outer solution* γ_0 *of the reduced problem* (2.5) *on the subsonic branch* S_0^{sub} *for* $r \in [r_0, r_i]$, *and another outer solution* γ_1 *of the reduced problem* (2.5) *on the supersonic branch* S_1^{super} *for* $r \in [r_i, r_1]$ *starting at the sonic fold of* S_1 *for* $r = r_i$.

If $\varepsilon_0 > 0$ *is sufficiently small, then for all* $\varepsilon \in (0, \varepsilon_0)$ *there exists a standing wave solution* $\Gamma^s(\varepsilon)$ *of system* (2.3) *lying within* $O(\varepsilon^{2/3})$ *of* Γ^s. *The boundary manifolds* B_j, $j = 0, 1$, *given by Definition* 4, *determine a unique subsonic-to-supersonic evaporation wave.*

Remark 5.5. The $O(\epsilon^{2/3})$ neighborhood statement in Theorem 5.3 is due to the boundary layer position near the sonic surface of S_1. This leads to a turning point problem in terms of classic matched asymptotic expansions.

Proof. Fenichel theory [16] implies that the trajectory $\gamma_0 \subset S_0^{sub}$ perturbs to $\gamma_0(\varepsilon) \subset S_0^{sub}(\varepsilon)$ and $O(\varepsilon)$ close to γ_0. We denote the end points of this segment $\gamma_0(\varepsilon)$ by $P_0(\varepsilon)$ at $r = r_0$ and $E_-^1(\varepsilon)$ at $r = r_i^\varepsilon$. Similarly, the segment of the trajectory $\gamma_1 \subset S_1^{super}$ which is bounded away from the sonic surface, i.e., for $r \in [r_i^\varepsilon + \eta, r_1]$ and $\eta > 0$, perturbs by Fenichel theory to $\gamma_1(\varepsilon) \subset S_1^{super}(\varepsilon)$ and $O(\varepsilon)$ close to γ_1. We denote the end points of this segment $\gamma_1(\varepsilon)$ by $P_1(\varepsilon)$ at $r = r_1$ and $P_\eta(\varepsilon)$ at $r = r_i^\varepsilon + \eta$. Furthermore, Fenichel theory implies that the manifolds $W^i(S_j^k)$, $i = s, u$, $j = 0, 1$, and $k = sub, super$, perturb smoothly to $O(\varepsilon)$-close local manifolds $W^i(S_j^k(\varepsilon))$.

Recall that $\Phi(y, \varepsilon)$ denotes the flow of the nonlinear system (2.2) for $\varepsilon > 0$. Since the boundary manifold B_1 transversely intersects the unstable fibers $W^u(P_1(\epsilon))$, the backward image $B_1' = \Phi(r_i^\varepsilon + \eta - r_1, \varepsilon)B_1$ is C^1 close to the stable fiber at $P_\eta(\epsilon)$. This follows from the exchange lemma. Similarly, since the boundary manifold B_0 transversely intersects the stable fiber $W^s(P_0(\epsilon))$, the forward image $B_0' = \Phi(r_i^\varepsilon + r_0, \varepsilon)B_0$ is C^1 close to the unstable fibers $W^u(E_-^1(\varepsilon))$.

The aim of the rest of the proof is to track $\gamma_1(\varepsilon)$ and hence the manifold B_1' backward around the sonic surface of S_1 and towards the subsonic branch S_0^{sub} to show that the image transversely intersects with B_0' at $r = r_i^\varepsilon$. A similar analysis is presented in [2] in the context of electrical waves in cardiac tissue that are modeled by a reaction-diffusion system. The proof is divided into three parts. In Parts A and B, we study the local dynamics near the sonic surface of S_1. This enables us to track, in Part C, the boundary manifold of the supersonic branch S_1^{super} ("backward") towards the subsonic branch S_0^{sub}, to show the transverse intersection of the boundary manifolds and hence the existence of a unique subsonic-to-supersonic wave.

5.2.1. Part A: Isolating the nonhyperbolic dynamics near the sonic surface of S_1. At the sonic surface of S_1 one of the nonzero eigenvalues of the layer problem, l_1, becomes zero, which corresponds to an eigenvector tangent to the u-axis. Normal hyperbolicity is lost along the sonic surface, i.e., each singularity on the sonic surface has a zero eigenvalue of algebraic multiplicity four, and Fenichel's theory does not apply anymore. To be able to extend the slow manifold $S_1^{super}(\varepsilon)$ and its foliation (backward) into the neighborhood of the sonic surface of S_1, we apply the *blow-up technique* [7, 21, 32] in the neighborhood of the sonic surface.

This geometric technique is commonly used to prove complex oscillatory behavior in singularly perturbed systems.

To be able to apply the blow-up technique, we have to isolate first the nonhyperbolic dynamics locally near the sonic surface of S_1 which are constrained to a four-dimensional center manifold W^c. The corresponding generalized center eigenspace E^c is spanned by the basis of the coordinates (r, m, n, u). Hence, the four-dimensional invariant center manifold W^c is a graph over the basis of the coordinates (r, m, n, u). In fact, the center manifold W^c is defined by $\lambda = 1$, $\theta = 0$ since this defines a four-dimensional invariant subspace of (2.3) for $\varepsilon \geq 0$ and the flow on W^c is given by

$$\begin{aligned} r_z &= \epsilon, \\ m_z &= -\epsilon\frac{2m}{r}, \\ n_z &= \epsilon\frac{2mu}{r}, \\ u_z &= n + mu + p\left(1, \frac{m}{u}\right) - \epsilon\frac{2u}{r} =: f(r, m, n, u, \varepsilon)\,. \end{aligned} \tag{5.2}$$

PROPOSITION 5.1. *For $m, r, u > 0$, there exists a smooth change of coordinates that transforms system* (5.2) *locally near the sonic surface of S_1 to*

$$\begin{aligned} \tilde{r}_z &= \epsilon O(\tilde{n}, \tilde{u}) =: \varepsilon\tilde{g}_3(\tilde{r}, \tilde{m}, \tilde{n}, \tilde{u}), \\ \tilde{m}_z &= \epsilon O(\tilde{n}, \tilde{u}) =: \varepsilon\tilde{g}_2(\tilde{r}, \tilde{m}, \tilde{n}, \tilde{u}), \\ \tilde{n}_z &= -\epsilon(M_1(\tilde{m}) + O(\tilde{n}, \tilde{u})) =: \varepsilon\tilde{g}_1(\tilde{r}, \tilde{m}, \tilde{n}, \tilde{u}), \\ \tilde{u}_z &= \tilde{n} + M_2(\tilde{m})\tilde{u}^2 + O(\epsilon, \tilde{n}\tilde{u}^2, \tilde{u}^3) =: \tilde{f}(\tilde{r}, \tilde{m}, \tilde{n}, \tilde{u}), \end{aligned} \tag{5.3}$$

where $M_1(\tilde{m}) > 0$ and $M_2(\tilde{m}) > 0$ for $\tilde{m} > 0$.

Proof. System (5.2) is a singularly perturbed system with three slow variables (r, m, n) and one fast variable u and has a three-dimensional folded critical manifold S_1 (2.8) given by $n = N(m, u) = -mu - p(1, \frac{m}{u})$. The sonic surface is defined by $f_u = \frac{m}{u^2}(u^2 - p_\rho) = 0$. Since

$$f_{uu} = \frac{m^2}{u^4}p_{\rho\rho} + \frac{2m}{u^3}p_\rho > 0 \quad \forall m, u > 0$$

it follows by the implicit function theorem that the sonic surface equation $f_u = 0$ can be solved for $u = U(m)$, i.e., the sonic surface is a graph over (r, m)-space (although independent of r). The coordinate transformation

$$\tilde{n} = n - N(m, U(m))\,, \qquad \tilde{u} = u - U(m) \tag{5.4}$$

rectifies the sonic surface to its base, the (r, m)-space. After applying the Taylor expansion of $p(1, \frac{m}{u})$ at $\tilde{u} = 0$, we arrive at system

$$\begin{aligned} r_z &= \epsilon, \\ m_z &= -\epsilon\frac{2m}{r} =: \varepsilon g_2(r, m), \\ \tilde{n}_z &= -\epsilon(M_1(m) + O(\tilde{u})) =: \varepsilon g_1(r, m, \tilde{u}), \\ \tilde{u}_z &= \tilde{n} + M_2(m)\tilde{u}^2 + O(\epsilon, \tilde{u}^3), \end{aligned} \tag{5.5}$$

where

$$M_1(m) := \frac{2m}{r}\,U(m) > 0\,, \qquad M_2(m) := \frac{1}{2}(\rho_u^2\, p_{\rho\rho} + \rho_{uu}\, p_\rho) > 0. \tag{5.6}$$

To prove M_1 and M_2 are positive, we observe that $\rho = m/u$ so that $\rho_{uu} = \frac{2m}{u^3} > 0$ for $m, u > 0$ and $p_\rho, p_{\rho\rho} > 0$ by (1.2). In a last step we apply the transformation

$$\tilde{r} = r - \frac{1}{g_1(m,r,0)}\tilde{n}\,, \qquad \tilde{m} = m - \frac{g_2(m,r)}{g_1(m,r,0)}\tilde{n} \tag{5.7}$$

and the Taylor expansion along the sonic surface to obtain the result. □

System (5.3) is a normal form of a singularly perturbed system with a three-dimensional folded critical manifold. The point E^+ on the folded surface F satisfies the *transversality condition*

$$\left.\begin{pmatrix} \tilde{f}_{\tilde{r}} \\ \tilde{f}_{\tilde{m}} \\ \tilde{f}_{\tilde{n}} \end{pmatrix} \cdot \begin{pmatrix} \tilde{g}_3 \\ \tilde{g}_2 \\ \tilde{g}_1 \end{pmatrix}\right|_{E^+ \in F} \neq 0, \tag{5.8}$$

which is also known as the *normal switching condition*. Recall that the reduced flow of (5.3) is away from the folded surface. Hence $E^+ \in F$ is a regular jump point for the backward flow of (5.3). In fact, any point on F has this property. Note that $\tilde{f}(\tilde{r}, \tilde{m}, 0, 0) = 0$ defines the sonic surface F.

5.2.2. Part B: Transition map and the blow-up. Note that the center manifold W^c itself is normally hyperbolic. Hence its two-dimensional foliation perturbs smoothly for $0 < \varepsilon \ll 1$. This result includes, in particular, the one-dimensional stable foliation which is an important observation, since we are interested in extending the supersonic manifold $S_1^{super}(\varepsilon)$ and its stable foliation into the neighborhood of the sonic surface F (and beyond). If we are able to track the position of the base points of these fibers, then we know how to track the corresponding stable foliation. This defines the aim of this section, i.e., to track the base points in the center manifold W^c.

For small $d > 0$, we define a transition map $\Pi : \Delta_{out} \to \Delta_{in}$ for the backward flow of (5.3) where

$$\Delta_{out} = \{(\tilde{r}, \tilde{m}, -d^2, \tilde{u}) : (\tilde{r}, \tilde{m}, \tilde{u}) \in J_{out}\} \tag{5.9}$$

is a section transverse to the supersonic branch S_1^{super}, where $J_{out} \in \mathbb{R}^3$ is a suitable domain, and

$$\Delta_{in} = \{(\tilde{r}, \tilde{m}, \tilde{n}, -d) : (\tilde{r}, \tilde{m}, \tilde{n}) \in J_{in}\} \tag{5.10}$$

is a section transverse to the fast fibers, where $J_{in} \in \mathbb{R}^3$ is a suitable domain.

PROPOSITION 5.2. *For system* (5.3) *there exists an* $\varepsilon_0 > 0$ *such that for* $\varepsilon \in (0, \varepsilon_0)$ *the following hold:*

1. *There exists a suitable rectangle* I_{in} *such that for* $(\tilde{r}, \tilde{m}) \in I_{in}$ *the manifold* $S_1^{super}(\varepsilon)$ *intersects* Δ_{in} *in a smooth surface which is a graph* $\tilde{n} = h_{in}(\tilde{r}, \tilde{m}, \varepsilon)$.
2. *The section* Δ_{out} *is mapped to an exponentially thin strip around* $S_1^{super}(\varepsilon) \cap \Delta_{in}$, *i.e., its width in* $\tilde{n}$ *direction is* $O(e^{-k/\varepsilon})$ *where* k *is a positive constant.*
3. *The map* $\Pi : \Delta_{out} \to \Delta_{in}$ *has the form*

$$\Pi \begin{pmatrix} \tilde{r} \\ \tilde{m} \\ \tilde{u} \end{pmatrix} = \begin{pmatrix} G_r(\tilde{r}, \tilde{m}, \tilde{u}, \varepsilon) \\ G_m(\tilde{r}, \tilde{m}, \tilde{u}, \varepsilon) \\ h_{in}(G_r(\tilde{r}, \tilde{m}, \tilde{u}, \varepsilon), G_m(\tilde{r}, \tilde{m}, \tilde{u}, \varepsilon), \varepsilon) + O(e^{-k/\varepsilon}) \end{pmatrix}, \tag{5.11}$$

with $h_{in}(G_r(\tilde{r}, \tilde{m}, \tilde{u}, \varepsilon), G_m(\tilde{r}, \tilde{m}, \tilde{u}, \varepsilon), \varepsilon) = O(\varepsilon^{2/3})$, $G_x(\tilde{r}, \tilde{m}, \tilde{u}, \varepsilon) = G_{x,0}(\tilde{x}) + O(\varepsilon \ln \varepsilon)$, $x = r, m$, *where* $G_{x,0}(\tilde{x}) = \tilde{x} + O(d^3)$ *is induced by the (backward) reduced flow on* S_1^{super} *from* Δ_{out} *to the fold surface* F.

Proof. This is an extension of the proof of Theorem 1 presented in [32] that studied singularly perturbed systems with two-dimensional folded critical manifold consisting of regular jump points. The increase of dimension of the folded critical manifold does not change the nature of the blow-up analysis presented in [32]. In fact, the above result can be extended to any l-dimensional folded critical manifold, $l \geq 2$, that consists of regular jump points. In section 6 we present the basic concept of the (rather lengthy) proof and refer to [32] for details. □

The local result of the transition map Π in Proposition 5.2 has been obtained after preliminary transformations of system (5.2) to system (5.3) by a local diffeomorphism. Hence there exists a section $\tilde{\Delta}_{in}$, respectively, $\tilde{\Delta}_{out}$, in system (5.2), which is the preimage of Δ_{in}, respectively, Δ_{out}, in system (5.3). Without loss of generality, let us assume that the parameter $d > 0$ that defines Δ_{in}, respectively, Δ_{out}, and the parameter η that defines $r = r_i^{\varepsilon} + \eta$ are chosen in a way such that $\gamma_1(\varepsilon)$, viewed as a trajectory of system (5.2), crosses $\tilde{\Delta}_{out}$ for $r = r_i^{\varepsilon} + \eta$ and $\tilde{\Delta}_{in}$ for $r = r_i^{\varepsilon}$.

Thus the transition map Π tells us how to track $\gamma_1(\varepsilon)$ from the section $\tilde{\Delta}_{out}$ backward around the fold surface F and gives us its position in the section $\tilde{\Delta}_{in}$. Recall that the manifold B_1' is C^1 close to the stable fiber at $P_\eta(\varepsilon)$. Hence, the manifold B_1' will track (backward) C^1 close the unstable fiber along $\gamma_1(\varepsilon)$ to section $\tilde{\Delta}_{in}$,[2] and we denote this manifold by B_1''. So, based on the above analysis we see that on leaving the neighborhood of the fold F at $\tilde{\Delta}_{in}$, the tangent plane to $W^s(\gamma_1(\varepsilon))$ is spanned by a vector tangent to the (fast) stable fiber of the center manifold and a vector in the direction of the flow. By Proposition 5.2, $\gamma_1(\varepsilon)$ is $O(\varepsilon^{2/3})$ close to the unperturbed γ_i and, hence, the manifold $W^s(\gamma_1(\varepsilon))$ will be C^1 $O(\varepsilon^{2/3})$ close to the unperturbed one, and so will B_1''.

5.2.3. Part C: Transverse intersection of the tracked boundary manifolds. In Theorem 3.3 we have shown that there exists a unique subsonic-to-sonic evaporation layer solution γ_i connecting the base point $E_-^1 \in S_0^{sub}$ to $E_+ \in F \subset S_1$ on the sonic surface, i.e., the corresponding layer fiber intersection $W^u(E_-^1) \cap W^{cs}(E_+) = \gamma_i$ is transverse. This unique solution γ_i is C^1 close to the center direction of E_+. In Part B we found that $W^s(\gamma_1(\varepsilon))$ is C^1 $O(\varepsilon^{2/3})$ close to $W^{cs}(E^+)$.

COROLLARY 5.1. *The reduced flow on the subsonic branch S_0^{sub} is transverse to the projection of the sonic surface F of S_1 onto S_0^{sub} along the unstable layer fibers of S_0^{sub}.*

Corollary 5.1 guarantees that the projection of $\gamma_1(\varepsilon) \subset S_1^{super}(\varepsilon)$ can be traced uniquely in an $O(\varepsilon^{2/3})$ neighborhood of γ_i toward $\gamma_0(\varepsilon) \subset S_0^{sub}(\varepsilon)$.

We are able to identify a fast fiber of $S_0^{sub}(\varepsilon)$ that has $\gamma_i(\varepsilon)$ on it at $\tilde{\Delta}_{in}$ and the corresponding base point on $S_0^{sub}(\varepsilon)$ is $E_-^1(\varepsilon)$. The corresponding unstable manifold $W^u(E_-^1(\varepsilon))$ is C^1 $O(\varepsilon)$ close to $W^u(E_-^1)$. Hence, B_0' is C^1 $O(\varepsilon)$ close to $W^u(E_-^1)$. The transverse intersection $W^u(E_-^1) \cap W^{cs}(E_+)$ and the sufficiently small perturbation $0 < \varepsilon \ll 1$ imply the transverse intersection of B_0' and B_1''. Thus a unique subsonic-to-supersonic evaporation wave $\Gamma^s(\varepsilon)$ has been found that is within an $O(\varepsilon^{2/3})$ neighborhood of Γ^s. The proof of Theorem 5.3 is complete. □

6. Outline of proof of Proposition 5.2. Since normal hyperbolicity of the critical manifold S_1 is lost near the fold surface F, one has to use the blow-up technique [7, 21, 32] to analyze the flow near the fold. To be more precise, the blow-up analysis is applied to the extended system $\{(5.3), \varepsilon_z = 0\}$. We define the blow-up transformation

[2] To be more precise: to section $\tilde{\Delta}_{in} \times (\lambda, \theta)$.

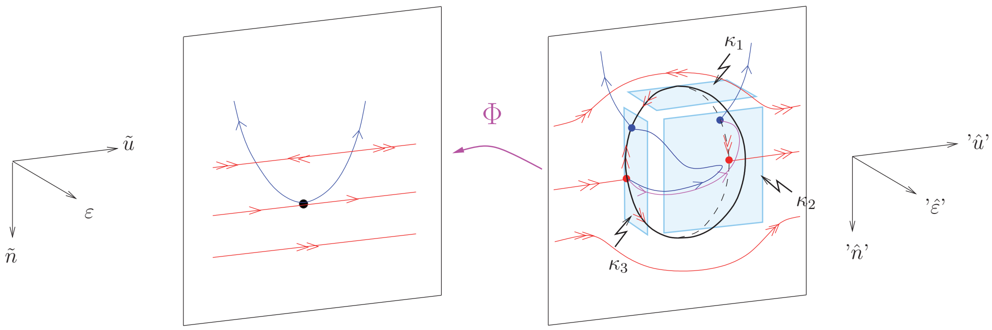

FIG. 11. *A sketch of the action of the* blow-up Φ. *The sonic surface of S_1 (here a black dot, left) is blown up to a half-cylinder (here a half-sphere, right). Three charts are needed (κ_1–κ_3, right) to cover the essential flow in the blown-up locus.*

$\Phi : \mathbb{S}^2 \times \mathbb{R}^3 \to \mathbb{R}^5$,

$$\tilde{n} = \delta^2 \hat{n}\,, \quad \tilde{u} = \delta \hat{u}\,, \quad \varepsilon = \delta^3 \hat{\varepsilon}\,, \tag{6.1}$$

where $\delta \geq 0$ represents the "radial" component of the blow-up. This leads to a blow-up manifold $\mathbb{S}^2 \times \mathbb{R}^3$ with $(\hat{n}, \hat{u}, \hat{\varepsilon}) \in \mathbb{S}^2$, i.e., the fold surface F is blown up to a cylinder $\mathbb{S}^2 \times J$ with $(\tilde{r}, \tilde{m}) \in J$. Figure 11 shows the action of the blow-up Φ; namely, it inflates the singularity (black dot, left) to a two-sphere (compact object, right). Note that this *cylindrical* blow-up Φ acts only transverse to the sonic surface (the fold), which indicates that this procedure is independent of the dimension l of the fold.[3]

In the extended phase space of $\{(5.3), \varepsilon_z = 0\}$ the slow manifold $S_1^{super}(\varepsilon)$ corresponds to a slice $\varepsilon =$ const. of a four-dimensional (supersonic) slow manifold which we denote by M_1 (see Figure 12, left). With the blow-up technique, we are able to extend this four-dimensional manifold (denoted $\hat{M}_1$ in the blow-up) near the sonic surface backward onto the blown-up sphere, and we are able to show that this manifold $\hat{M}_1$ exits the blown-up sphere almost parallel to the "center fibers," as shown in Figure 12. This is possible, because we have gained normal hyperbolicity at both branches of S_1 at the equator as indicated by double arrows near $\hat{E}_+^1$ and $\hat{E}_2^+$ in Figure 12.

To rigorously calculate the extension of $\hat{M}_1$ by the (backward) flow on the upper blown-up cylinder, one would need three charts, denoted κ_1 to κ_3, to cover the essential flow on the cylinder. These charts are defined by $\kappa_1 : \hat{n} = -1$, $\kappa_2 : \hat{\varepsilon} = 1$, and $\kappa_3 : \hat{u} = -1$ (see Figure 11). We do not present a full blow-up analysis here, which can be found in [32], but show only the core of the analysis, which is covered by chart κ_2. In this chart, the blow-up is simply an ϵ-dependent rescaling of the dependent variables $\tilde{n} = \epsilon^{2/3}\hat{n}$, $\tilde{u} = \epsilon^{1/3}\hat{u}$ and the independent variable $z = \epsilon^{-1/3}\zeta$, which transforms (5.3) to

$$\begin{aligned} \tilde{r}' &= O(\epsilon), \\ \tilde{m}' &= O(\epsilon), \\ \hat{n}' &= -M_1(\tilde{m}) + O(\epsilon^{1/3}), \\ \hat{u}' &= \hat{n} + M_2(\tilde{m})\hat{u}^2 + O(\epsilon^{1/3}). \end{aligned} \tag{6.2}$$

[3]This points to the generality of the blow-up analysis presented in [32].

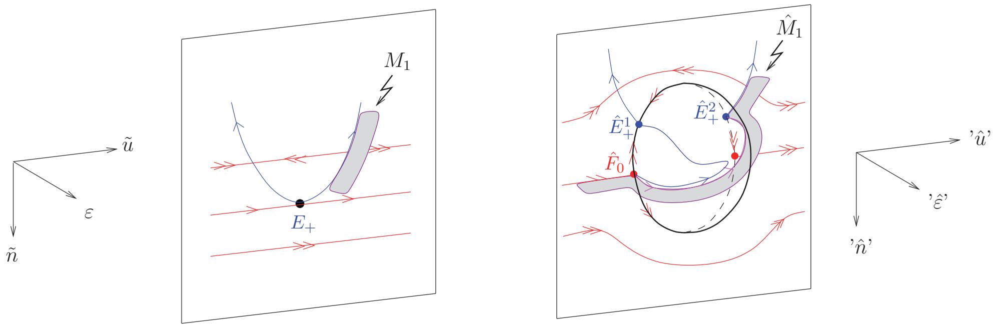

FIG. 12. *A sketch of the supersonic slow manifold M_1 of the extended system $\{(5.3), \varepsilon_z = 0\}$ in $(\tilde{u}, \tilde{n}, \varepsilon)$-space (left). The blow-up of the region near the fold surface (black-dot, left) and a sketch of the extension of the slow (blown-up) manifold $\hat{M}_1$ over the blown-up sphere (right).*

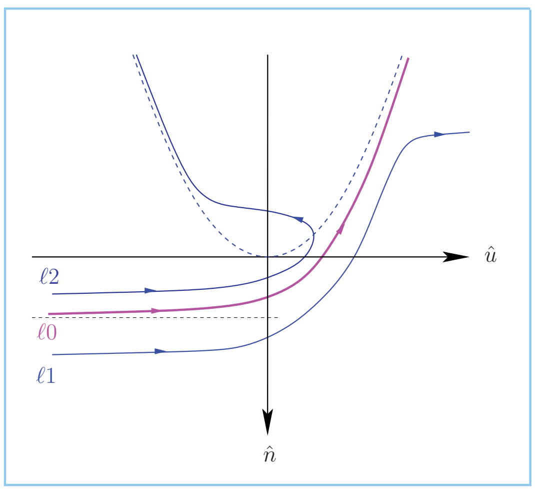

FIG. 13. *The local flow near the sonic surface of S_1 is given by a Riccati equation* (6.3). *It represents the flow in chart κ_2 shown in Figure* 11. *The pink curve ℓ_0 connects to the supersonic branch of S_1 at the equator of the blown-up sphere (to E_+^2 in Figure* 12*).*

Note that system (6.2) is a regularly perturbed system (on a compact domain) since $M_1 > 0$ by (5.6). As $\varepsilon^{1/3} \to 0$, this yields system

$$\begin{aligned} \hat{n}' &= -M_1(\tilde{m}), \\ \hat{u}' &= \hat{n} + M_2(\tilde{m})\hat{u}^2, \end{aligned} \tag{6.3}$$

which is known as a Riccati equation (see, e.g., [29]). Since we are dealing with a regular perturbation problem (on a compact domain), this also implies that the local dynamics of (5.3) are governed (to leading order) by the Riccati equation (6.3) in a region where $(\tilde{n}, \tilde{u})$ are $O(\epsilon^{2/3}) \times O(\epsilon^{1/3})$.

The dynamics of system (6.3) are well studied (see, e.g., [29]), and Figure 13 shows a phase portrait of the Riccati flow. Note that "infinity" in chart κ_2 corresponds to the "equator" of the blown-up sphere (see Figure 11). Thus, the flow in Figure 13 can be divided into three types depending on how the Riccati flow connects to the equator of the blown-up sphere:

1. There exists a unique solution $\ell_0(\zeta)$ (shown in pink) that approaches the "positive" branch ($\hat{u} > 0$) of the parabola $\hat{n} + M_2(\tilde{m})\hat{u}^2 = 0$ as $\zeta \to \infty$. This solution connects asymptotically to the supersonic branch S_1^{super} at the equator of the blown-up sphere (to $\hat{E}_+^2$ in Figure 12).
2. There is a one-dimensional family of solutions $\ell_1(\zeta)$ whose $\hat{u}$ coordinate becomes unbounded ($+\infty$) as $\zeta \to \infty$. These solutions connect asymptotically to the (fast) outgoing center fiber at the equator of the blown-up sphere.
3. There is a one-dimensional family of solutions $\ell_2(\zeta)$ that approaches the "negative" branch ($\hat{u} < 0$) of the parabola $\hat{n} + M_2(\tilde{m})\hat{u}^2 = 0$ as $\zeta \to \infty$. All these solutions connect asymptotically to the subsonic branch S_1^{sub} at the equator of the blown-up sphere (to $\hat{E}_+^1$ in Figure 12).

All three types of solutions connect in backward "time" to the (fast) incoming center fiber at the equator of the blown-up sphere (to $\hat{F}_0$ in Figure 12).

Note further that system (6.2) has an intermediate $O(\varepsilon^{1/3})$ scale. Thus chart κ_2 corresponds to a matching region of an inner solution (chart κ_3, fast $O(1)$ scale) and an outer solution (chart κ_1, slow $O(\varepsilon)$ scale) of this "turning point" problem. The flow in the rescaling chart κ_2 indicates how the manifold $\hat{M}_1$ and hence the manifold $S_1^{super}(\varepsilon)$ can be extended from the supersonic regime around the sonic surface F and how it then exits almost parallel to the ("fast") center fibers. It also hints to the $O(\varepsilon^{2/3})$ displacement stated in Proposition 5.2 due to the different weights (powers of ϵ) of the blow-up transformation, which is well known for this type of turning point problem. The details of the entry and the exit of the manifold $S_1^{super}(\varepsilon)$ near the blown-up cylinder are covered by the dynamics in the entry and exit charts κ_1 and κ_3. As mentioned before, we omit the corresponding analysis in these charts. It can be found in [32].

Remark 6.1. The result of Proposition 5.2 is independent of the choice of $S_1^{super}(\varepsilon)$; see also Remark 5.1.

7. Concluding remarks. To the best of our knowledge, this paper proves for the first time the existence of transonic evaporation waves in a spherically symmetric nozzle. The key in proving the existence of these evaporation waves is the application of recent results and techniques within the field of dynamical systems. In the case of supersonic-to-subsonic evaporation waves, a generalization of the *exchange lemma* [19] is needed that deals with a node-to-saddle transition that describes the evaporation layer. This *generalized exchange lemma* was recently shown in the case of the Fisher-KPP equation [25].

In the case of subsonic-to-supersonic evaporation waves, the application of a geometric desingularization technique, known as the *blow-up technique* [32], is needed to deal with loss of normal hyperbolicity near the sonic surface. This blow-up technique was also successfully used in a different physical context to prove the existence of electrical waves in cardiac tissue that are modeled by a reaction-diffusion system [2].

It is worthwhile to mention the deep insights one can gain from this geometric desingularization procedure. The blow-up technique allows us to identify the preimages of solutions in a small neighborhood of the sonic surface for $0 < \varepsilon \ll 1$, which already exists on the blown-up cylinder for $\varepsilon = 0$. These are the solutions of the Riccati equation (6.3) in chart κ_2 compactified onto the blown-up cylinder, as schematically shown in Figure 12. They are connected to the sub- or supersonic branch of S_1.

For example, we are able to identify the preimages of the one-parameter family of supersonic-to-sonic evaporation layer solutions $E_-^2 \to E_+$ shown in Figure 8 locally near E_+. These are all solutions on the blown-up cylinder that connect from the fiber point $\hat{F}_0$ on the equator to the subsonic point $\hat{E}^1_+$ on the equator. These solutions correspond to the family of solutions ℓ_2 of the Riccati equation shown in Figure 13.

Note that the unique layer solution $E^2_- \to E_+$ shown in Figure 8 does not show up directly in the blow-up (Figure 12) because it is not part of the center manifold, i.e., it approaches the sonic point E_+ in a transverse direction to the center manifold. Obviously, we cannot identify the heteroclinic connection from E^2_- to E^1_- (wet shock, shown in Figure 8) in Figure 12 because none of the equilibria is part of the blow-up.

More importantly, we can also identify the preimages of the layer solutions shown in Figure 7 in the blow-up shown in Figure 12 as $n \to \bar{n}$: The limit of the subsonic evaporation wave $E^1_- \to E^1_+$ corresponds to the connection $\hat{F}_0 \to \hat{E}^1_+$ along the equator. The limit of the dry wave $E^1_+ \to E^2_+$ corresponds to the connection $\hat{E}^1_+ \to \hat{E}^2_+$ along the equator. Finally, the limit of the supersonic evaporation wave $E^2_- \to E^2_+$ can be thought of as a connection to $\hat{E}^2_+$ on the equator transverse to the center manifold. By continuity, the (local) solutions in the interior of Figure 7 near E^1_+ have preimages that correspond to solution ℓ_2 on the blown-up sphere.

REFERENCES

[1] G. K. Batchelor, *An Introduction to Fluid Dynamics*, Cambridge University Press, Cambridge, UK, 1967.

[2] M. Beck, C. K. R. T. Jones, D. Schaeffer, and M. Wechselberger, *Electrical waves in a one-dimensional model of cardiac tissue*, SIAM J. Appl. Dyn. Syst., 7 (2008), pp. 1558–1581.

[3] S. Canic, B. L. Keyfitz, and G. M. Lieberman, *A proof of existence of perturbed steady transonic shocks via a free boundary problem*, Comm. Pure Appl. Math., 53 (2000), pp. 484–511.

[4] G. Q. Chen, C. M. Dafermos, M. Slemrod, and D. H. Wang, *On two-dimensional sonic-subsonic flow*, Comm. Math. Phys., 271 (2007), pp. 635–647.

[5] S.-X. Chen, *Compressible flow and transonic shock in a diverging nozzle*, Comm. Math. Phys., 289 (2009), pp. 75–106.

[6] R. Courant and K. O. Friedrichs, *Supersonic Flow and Shock Waves*, Interscience, 1948.

[7] F. Dumortier, *Local study of planar vector fields: Singularities and their unfoldings*, in Structures in Dynamics, Finite Dimensional Deterministic Studies, H. W. Broer et al., eds., Stud. Math. Phys. 2, North-Holland, Amsterdam, 1991, pp. 161–241.

[8] P. J. Evans and J. C. Mackie, *Shock-wave interaction with an evaporating aerosol*, Phys. Fluids, 14 (1971), pp. 539–541.

[9] H. Fan, *Travelling waves, Riemann problems and computations of a model of the dynamics of liquid/vapour phase transitions*, J. Differential Equations, 150 (1998), pp. 385–437.

[10] H. Fan, *On a model of the dynamics of liquid/vapor phase transitions*, SIAM J. Appl. Math., 60 (2000), pp. 1270–1301.

[11] H. Fan, *Symmetry breaking, ring formation and other phase boundary structures in shock tube experiments on retrograde fluids*, J. Fluid Mech., 513 (2004), pp. 47–75.

[12] H. Fan and X.-B. Lin, *Collapsing and explosion waves in phase transitions with metastability, existence, stability and related Riemann problems*, J. Dynam. Differential Equations, 22 (2009), pp. 163–191.

[13] H. Fan and X.-B. Lin, *A dynamical systems approach to traveling wave solutions for liquid/vapor phase transition*, Fields Inst. Commun., 64 (2013), pp. 101–117.

[14] H. Fan and X.-B. Lin, *Standing waves in phase transitions in a spherically symmetric nozzle*, SIAM J. Math. Anal., 44 (2012), pp. 405–436.

[15] H. Fan and M. Slemrod, *Dynamic flows with liquid/vapor phase transitions*, in Handbook of Mathematical Fluid Dynamics, Vol. I, North-Holland, Amsterdam, 2002, pp. 373–420.

[16] N. Fenichel, *Geometric singular perturbation theory*, J. Differential Equations, 31 (1979), pp. 53–98.

[17] J. M. Hong, C.-H. Hsu, and W. Liu, *Viscous standing asymptotic states of isentropic compressible flows through a nozzle*, Arch. Ration. Mech. Anal., 196 (2010), pp. 575–597.

[18] J. M. Hong, C.-H. Hsu, and W. Liu, *Inviscid and viscous stationary waves of gas flow through contracting-expanding nozzles*, J. Differential Equations, 248 (2010), pp. 50–76.

[19] C. K. R. T. Jones, *Geometric singular perturbation theory*, in Dynamical Systems, Montecatini Terme, 1994, Lecture Notes in Math. 1609, Springer, Berlin, 1995, pp. 44–118.

[20] S. Kotake and I. I. Glass, *Flows with nucleation and condensation*, Prog. Aerospace Sci., 19 (1981), pp. 129–196.

[21] M. Krupa and P. Szmolyan, *Extending geometric singular perturbation theory to nonhyperbolic points—fold and canard points in two dimensions*, SIAM J. Math. Anal., 33 (2001), pp. 286–314.

[22] P. D. Lax, *Hyperbolic systems of conservation laws* II, Comm. Pure Appl. Math., 10 (1957), pp. 537–566.

[23] J. Li, Z. P. Xin, and H. C. Yin, *The existence and monotonicity of a three-dimensional transonic shock in a finite nozzle with axisymmetric exit pressure*, Pacific J. Math., 247 (2010), pp. 109–162.

[24] X.-B. Lin, *Heteroclinic bifurcation and singularly perturbed boundary value problems*, J. Differential Equations, 84 (1990), pp. 319–382.

[25] X.-B. Lin, *Stability of standing waves for monostable reaction-convection equations in a large bounded domain with boundary conditions*, J. Differential Equations, 255 (2013), pp. 58–84.

[26] T.-P. Liu, *Nonlinear stability and instability of transonic flows through a nozzle*, Comm. Math. Phys., 83 (1982), pp. 243–260.

[27] W. Liu and M. Oh, *Instability of low density supersonic waves of a viscous isentropic gas flow through a nozzle*, in Infinite Dimensional Dynamical Systems, Fields Inst. Commun. 64, Springer, New York, 2013, pp. 169–183.

[28] A. Majda and R. Pego, *Stable viscosity matrices for systems of conservation laws*, J. Differential Equations, 56 (1985), pp. 229–262.

[29] E. F. Mishchenko and N. Kh. Rozov, *Differential Equations with Small Parameters and Relaxation Oscillations*, Plenum Press, New York, 1980.

[30] P. Roth and R. Fischer, *An experimental shock wave study of aerosol droplet evaporation in the transition regime*, Phys. Fluids, 28 (1985), pp. 1665–1672.

[31] G. S. Springer, *Homogeneous nucleation*, in Advances in Heat Transfer, Vol. 14, Academic Press, 1978, pp. 281–315.

[32] P. Szmolyan and M. Wechselberger, *Relaxation oscillations in* $\mathbb{R}^3$, J. Differential Equations, 200 (2004), pp. 69–104.

[33] P. A. Thompson, H. Chaves, C. E. Meier, Y.-G. Kim, and H.-D. Speckmann, *Wave splitting in a fluid of large heat capacity*, J. Fluid Mech., 185 (1987), pp. 385–414.

[34] M. Wechselberger and G. Pettet, *Folds, canards and shocks in advection-reaction-diffusion models*, Nonlinearity, 23 (2010), pp. 1949–1969.

[35] C. J. Xie and Z.P. Xin, *Global subsonic and subsonic-sonic flows through infinitely long nozzles*, Indiana Univ. Math. J., 56 (2007), pp. 2991–3023.

[36] Z. P. Xin, W. Yan, and H. C. Yin, *Transonic shock problem for the Euler system in a nozzle*, Arch. Ration. Mech. Anal., 194 (2009), pp. 1–47.